Regional centromeres protect organisms from lethal mutations

Sundar Ram Sankaranarayanan[1], Satyadev Polisetty[1], Arti Dumbrepatil[1], A. Arockia Jeyaprakash[2], Kaustuv Sanyal[1, *]

[1] Molecular Mycology Laboratory, Molecular Biology and Genetics Unit, Jawaharlal Nehru Centre for Advanced Scientific Research, Jakkur, Bengaluru 560064, India. [2]Wellcome Centre for Cell Biology, University of Edinburgh, Edinburgh EH9 3BF, UK

Email addresses of authors

SRS (sundar_ram@jncasr.ac.in), SP (pvssdev@jncasr.ac.in), AD (artidumbre@gmail.com), AAJ (jeyaprakash.arulanandam@ed.ac.uk), KS (sanyal@jncasr.ac.in)

*** Corresponding author**

Kaustuv Sanyal (sanyal@jncasr.ac.in)

Keywords

Microtubule binding, kinetochore microtubules, biorientation, CENPA nucleosome, mitosis

Abstract

Shorter centromeres have fewer kinetochore microtubules (kMTs) bound as evident in *Saccharomyces cerevisiae* where each chromosome is associated with a single kMT. Cells can also be conditioned in recruiting excess kMTs highlighting the flexibility of the kinetochore as the kMT binding interface. Here, we addressed the evolutionary significance of the inherent flexibility in conditionally recruiting excess kMTs. We identified a conserved arginine residue at the C-terminus of an essential outer kinetochore protein Dad2 that remained positively selected for ~700 million years in fungi. While the conserved R126 residue in Dad2 is essential for viability in *S. cerevisiae* harboring short point centromeres, the corresponding arginine residues are functionally important but no longer essential for viability in either *Candida albicans* or *Cryptococcus neoformans*, each possessing longer regional centromeres. We revealed a gradual decline in the requirement of the conserved arginine for chromosome biorientation and mitotic progression with increasing centromere length. Finally, our results suggested that the mutational tolerance in organisms with regional centromeres is imparted by higher kinetochore protein levels known to recruit multiple kMTs per chromosome.

Introduction

Accurate segregation of duplicated genetic material requires dynamic and regulated attachment of the sister chromatids to spindle microtubules (MTs). This association is mediated by the kinetochore, a multiprotein complex that assembles on the centromeric locus on every chromosome (Cheeseman 2014). The centromere-specific histone H3 variant, CENPA (Cse4 in yeast), is a hallmark of functional centromeres and acts as the foundation for assembling other kinetochore proteins in most organisms (Cheeseman 2014; Musacchio and Desai 2017). The kinetochore ensemble spans 125 bp on each point centromeres of *Saccharomyces cerevisiae* and forms a single MT-binding module. Kinetochores on the longer regional centromeres of most other fungi and metazoans are considered as an array of the module formed on the point centromeres (Joglekar et al. 2006; Joglekar et al. 2008; Weir et al. 2016; Musacchio and Desai 2017; Walstein et al. 2021). This enables the large regional centromeres to support the binding of multiple MTs on each chromosome against a single MT binding to an *S. cerevisiae* chromosome (Ding et al. 1993; Winey et al. 1995). The underlying principle that determines the number of MTs to be associated with a chromosome remains unanswered.

The structural plasticity of a kinetochore plays a significant role in maintaining dynamic interactions with the associated kinetochore MTs (kMTs) across mitotic cell cycle. A well-known example highlighting this plasticity is the presence of multiple pathways linking the inner and outer layers of the kinetochore (Milks et al. 2009; Schleiffer et al. 2012; Hornung et al. 2014; Dimitrova et al. 2016; Sridhar et al. 2021). The anaphase enrichment of kinetochore subunits such as Ndc80 on a minimal kinetochore formed initially to satisfy the mitotic checkpoint highlights the temporal dynamicity within the kinetochore ensemble as cells progress through mitosis (Malvezzi et al. 2013; Dhatchinamoorthy et al. 2017; Dhatchinamoorthy et al. 2019). Besides these natural scenarios, flexibility in the ability to seed and form additional kMTs has also been demonstrated in engineered stains. For instance, over 50 copies of centromeric plasmids could be tolerated in *S. cerevisiae* as additional MTs formed to bind to the kinetochores assembled on these plasmids (Nannas et al. 2014). In another ascomycete *Candida albicans*, overexpression of CENPA resulted in the recruitment of excess outer kinetochore subunits on each centromere (Burrack et al. 2011). These molecules now act as receptors to bind multiple kMTs on each chromosome as opposed to a single kMT binding to each 3-5 kb long regional centromere in a

wild-type *C. albicans* cell. It remains unknown if this inherently plastic nature of the kinetochore protects organisms when exposed to extraneous stresses and acts as a natural failsafe mechanism to maintain high fidelity chromosome segregation.

The Ndc80 complex of the outer kinetochore forms the primary MT-binding arm of the kinetochore ensemble, with the Ndc80 and Nuf2 subunits forming direct contacts with the tubulin subunits. The load-bearing ability of the Ndc80 complex under tension is augmented by another fungus-specific outer kinetochore protein complex, the Dam1 complex (Lampert et al. 2010; Tien et al. 2010; Lampert et al. 2013). This heterodecameric complex, comprising of Dad1, Dad2, Dad3, Dad4, Dam1, Duo1, Ask1, Hsk3, Spc19, and Spc34 subunits, localizes explicitly to the kinetochore in an Ndc80-dependent manner and is essential for sister kinetochores to establish and maintain a bioriented state until anaphase onset (Hofmann et al. 1998; Cheeseman et al. 2001a; Cheeseman et al. 2001b; Enquist-Newman et al. 2001; Janke et al. 2002; Li et al. 2002). Consistently, mutants of the Dam1 complex subunits show severe chromosome segregation defects in all organisms studied to date (Hofmann et al. 1998; Enquist-Newman et al. 2001; Janke et al. 2002; Liu et al. 2005; Thakur and Sanyal 2011; Chatterjee et al. 2016; Sridhar et al. 2021).

The Dam1 complex is not only essential for viability in organisms with point or short regional centromeres that bind only one MT on each chromosome but also in a basidiomycete *Cryptococcus neoformans* that harbors long centromeric chromatin (Yadav et al. 2018; Sridhar et al. 2021). In this study, we attempted to understand functional significance of the length of centromeric chromatin and the MTs associated with each chromosome by studying Dad2, a subunit of the Dam1 complex, across organisms that diverged from each other more than 700 million years ago (van Hooff et al. 2017). We identified a conserved domain, named it the Dad2 signature sequence (DSS), at the C-terminus of Dad2 that contains an evolutionarily conserved arginine residue. Functional analysis of the DSS reveals that the conserved arginine residue is essential for viability and is required for chromosome biorientation and mitotic progression in *S. cerevisiae*, but a similar substitution of the corresponding arginine residue in organisms with longer centromeric chromatin could be tolerated to a varying extent.

Results

The Dad2 Signature Sequence (DSS) is a conserved motif at the C- terminus in the Dad2 protein family

The Dad2 protein family is typically defined by the presence of the Dad2 domain (PF08654), a conserved amino acid sequence stretch at the N- terminus (Figure 1A, *top).* To further understand the domain architecture, we analyzed the primary amino acid sequence of Dad2 from more than 500 fungal species collectively representing the three major fungal phyla- Ascomycota, Basidiomycota, and Mucoromycota (See Methods). Our multiple sequence alignment identified a 10-amino acid-long evolutionarily conserved sequence motif towards the C- terminus of Dad2 that we named the Dad2 signature sequence (DSS) (Figure 1A). The DSS motif remains conserved across species with diverse centromere structures known among fungi. While the extent of conservation of most amino acid residues is variable, the DSS possesses an almost invariant arginine residue (R') (Figure 1A). Further analysis of the DSS within specific fungal phyla revealed other features associated with this motif. Among the members of Saccharomycotina, the second position from the invariant arginine was also encoded by a positively charged amino acid such as arginine (R) or lysine (L) in low frequency. However, this position was predominantly represented by proline (P) in other fungal orders such as Pezizomycotina, Taphrinomycotina, and in the fungal phylum of Basidiomycota. Across species, we find the conserved arginine R' centered on a short hydrophobic patch. Interestingly, in the available three-dimensional structure of the Dam1 complex (PDB:6CFZ) (Jenni and Harrison 2018), the DSS motif makes multipartite interactions with residues of Dam1, Spc19, and Spc34 subunits within the 'central domain', suggesting its potential contribution to the overall structure and function of the Dam1 complex (Figure 1B). Particularly, the conserved arginine residue makes both hydrophobic and electrostatic interactions with residues of Spc19. Considering this together with our observation that the DSS motif is extensively conserved across the three major fungal phyla, we sought to understand the functional significance of this domain in Dad2, especially its conserved arginine residue in two fungal systems - *S. cerevisiae* and *C. albicans*, diverged from each other 117 mya (Shen et al. 2018), and known to possess distinct centromere structures and kinetochore architectures.

The functional importance of the DSS is correlated inversely to the centromere length

To study the DSS function in *S. cerevisiae*, we generated constructs expressing mutant versions of Dad2 bearing alanine substitutions of the conserved arginine residues or a truncated version lacking the entire DSS domain (ScDad2-R126A, ScDad2-R128A, and ScDad2-ΔDSS; Figure 1C). To test the function of these mutants, we used a previously reported temperature-sensitive (*ts*) mutant of *DAD2* wherein the genomic allele of *DAD2* was deleted and a *ts* allele was reintegrated (CJY077, *dad2*::*KanMX6 his3Δ200 leu2Δ1*::*pCJ055 (dad2^{ts})*) (Janke et al. 2002). This mutant strain was independently transformed with a pRS313-based *CEN/ARS* plasmid containing either wild-type or mutant versions of *DAD2* (as in Figure 1C) tagged with GFP at the C- terminus. In all these strains, the expression of *DAD2-GFP* was driven by the native promoter of Sc*DAD2*. The functional significance of each of these residues was tested by a spot dilution assay to determine the ability of the mutants to support growth at an elevated temperature of 37°C (Figure 1D). As expected, the strain YSR01 carrying the empty vector was unable to grow at this temperature, but the strain YSR02 expressing ScDad2-FL grew well. The strain YSR04 expressing ScDad2-R128A also supported growth at an elevated temperature, suggestive of a non-essential role of R128 for viability. Strikingly, the strains YSR03 expressing ScDad2-R126A and YSR05 expressing ScDad2-ΔDSS failed to grow at 37°C, revealing that R126 makes the DSS essential for Dad2 function in *S. cerevisiae*. To rule out the lack of expression of these mutant proteins as a cause for their inability to complement growth at an elevated temperature, we confirmed the localization of the ectopic Dad2 protein (wild-type, mutant, or truncated) at this temperature (Figure 1E). All versions of Dad2 except ScDad2-ΔDSS showed detectable punctate localization signals typical of clustered budding yeast kinetochores (Cheeseman et al. 2001b; Janke et al. 2002). These results strongly indicated that the DSS motif is essential for the kinetochore localization of ScDad2. Based on the location of the DSS in the Dam1 complex monomer, we suspect that the deletion of the entire DSS domain might affect the integrity of the complex and in turn the localization of Dad2.

To rule out the temperature sensitivity of mutant cells expressing ScDad2-R126A and ScDad2-ΔDSS observed in the above assay, we tested the essentiality of this residue at an ambient growth temperature (30°C) as well. A tester strain was engineered such that the genomic allele of Dad2 was deleted after expressing Dad2 from an ectopic allele cloned in a centromeric plasmid carrying the *URA3* gene (Figure S1A). This strain was then transformed with pRS313-based plasmids containing wild-type or mutant versions of *DAD2*. The ability of strains to lose the

protection allele present in the plasmid and support subsequent growth on media containing 5'FOA was used to test for the essentiality of the mutant Dad2 protein for viability. The inability of YSR10 expressing ScDad2-R126A and YSR12 expressing ScDad2-ΔDSS to grow on the Ura^+ counter-selection media containing 5'FOA at various dilutions tested in the spot dilution assay confirmed the essentiality of R126 and thereby the role of the DSS in cell viability (Figure S1A). These results confirmed that the highly conserved R126 residue is a critical amino acid for the essential function performed by Dad2 in *S. cerevisiae*.

Since ScDad2-R126A and ScDad2-ΔDSS mutants were inviable in *S. cerevisiae*, we sought to test the importance of the corresponding arginine residues in Dad2 that is essential for viability in *C. albicans*. To test this in *C. albicans*, we used a previously reported conditional mutant of *dad2* (J108, *dad2/PCK1pr-DAD2*) (Thakur and Sanyal 2011). In this conditional mutant, the only genomic allele of Ca*DAD2* is expressed under the *PCK1* promoter that shuts down its expression in the presence of dextrose in growth media (Figure S1B). While the conditional mutant J108 was unable to grow in media supplemented with dextrose, the complemented strains J108A and J108B expressing CaDad2-FL and CaDad2-ΔDSS respectively supported growth in this media, suggesting that unlike in *S. cerevisiae*, the deletion of the DSS motif is not lethal in *C. albicans* (Figure S1C). We further validated this observation by engineering the only allele of *DAD2* in ASR01 (*dad2/DAD2*) to express CaDad2-FL, -R92A, and -ΔDSS in strains ASR02, ASR03, and ASR04 respectively (Figure 1F). Spot dilution assays were performed to assess if any of the CaDad2 derivatives exhibited growth defects as compared to the wild-type strain. While we did not observe any significant growth retardation at 30°C, the growth of mutant strains ASR03 and ASR04 expressing CaDad2-R92A and CaDad2-ΔDSS respectively was significantly compromised at a lower temperature of 18°C when compared with CaDad2-FL expressing strain ASR02 or the wild-type strain SN148 grown under similar conditions (Figure 1G). We could detect punctate localization signals in strains expressing not only CaDad2-R92A but also CaDad2-ΔDSS, suggesting that kinetochore localization was neither affected by alanine substitution of the critical arginine residue nor even when the entire DSS was deleted in *C. albicans* (Figure 1H). These experiments reveal that the presence of the evolutionarily conserved arginine residue in Dad2 is not absolutely necessary for the viability of *C. albicans* under normal growth conditions. The severity of mutations in the DSS, however, was evident in the presence of stresses like low-temperature growth. Having observed such phenotypic differences in mutants of Dad2 in both

these species, we sought to further dissect the mutant phenotype to study the extent of functional conservation of the DSS between them.

The arginine residue R126 in the conserved DSS motif is critical for proper spindle dynamics and bipolar attachment of kinetochores in *S. cerevisiae*

To probe deeper into the role of the DSS and its conserved arginine R126 in chromosome segregation in *S. cerevisiae*, we generated conditional mutants of *DAD2* by replacing the endogenous *DAD2* promoter with the $GAL_{1\text{-}10}$ promoter in the strain SBY12503 where spindle pole bodies (Spc110 is tagged with mCherry) as well as *CEN3* are marked (by the binding of GFP-LacI to LacO arrays integrated adjacent to *CEN3*) (Umbreit et al. 2014). The resulting strain YSR13 (*GALpr-DAD2*) fails to grow when dextrose is the sole carbon source in the growth media (Figure S1D). This conditional mutant strain YSR13 was then independently transformed with vectors that reintegrate wild-type or mutant versions of *DAD2* expressed from the *DAD2* promoter at the native locus. In line with our previous observations, the conditional mutant complemented with ScDad2-FL in YSR14 and ScDad2-R128A in YSR16 supported growth on dextrose-containing media. On the other hand, the strains YSR15 and YSR17 expressing ScDad2-R126A and ScDad2-ΔDSS respectively could not complement function as they were unable to support the growth of the conditional mutant on this media (Figure S1E).

To identify the defects that led to viability loss, the *dad2* conditional mutant YSR13 along with the reintegrant strains YSR14 through YSR17 were grown for 8 h in dextrose-containing media to deplete Dad2 expressed under the *GAL* promoter. Post depletion, the cells were harvested and analyzed for cell cycle progression, spindle dynamics, and kinetochore-MT orientation (Figure 2A). Upon 8 h of growth in repressive media, flow cytometric analysis of propidium iodide-stained cells revealed the parent strain YSR13 (*GALpr-DAD2*) was arrested at the G2/M stage in line with previous observations (Figure 2B). The impaired MT-binding due to the lack of any Dam1 complex subunits is known to activate the spindle assembly checkpoint (SAC), resulting in the observed G2/M arrest. This arrest was rescued when the mutant was complemented with ScDad2-FL or ScDad2-R128A as observed in YSR14 and YSR16 respectively (Figure 2B). However, no rescue in the arrest was observed in strains YSR15 and YSR17 expressing ScDad2-R126A and ScDad2-ΔDSS respectively, suggesting the conserved arginine R126 in the DSS motif is essential for mitotic progression in *S. cerevisiae*.

At the same hour of Dad2 protein depletion, we examined the spindle dynamics using the fluorescently tagged spindle pole body protein, Spc110-mCherry, as the marker. In line with the metaphase arrest observed upon depletion of Dad2 in YSR13, we found these cells to have a short mitotic spindle (< 2 µm) (Figure 2C). The conditional mutant strain, when complemented with ScDad2-FL as in YSR14 or with ScDad2-R128A as in YSR16, was able to transit metaphase and enter anaphase, as suggested by an increased average spindle length of >2 µm (Figure 2C). We did not observe the rescue of the mitotic arrest and a corresponding increase in the spindle length when the same conditional mutant was complemented with ScDad2-R126A as in YSR15 or ScDad2-ΔDSS as in YSR17 (Figure 2C).

To validate if the observed defects were consequential of improper kinetochore-MT orientation at metaphase, we colocalized Spc110-mCherry with *CEN3*-GFP to monitor the nature of these attachments. Sister kinetochores were bioriented in majority of the cells in YSR14 expressing ScDad2-FL or YSR16 expressing ScDad2-R128A. By contrast, a significant proportion of YSR15 cells expressing ScDad2-R126A or YSR17 cells expressing ScDad2-ΔDSS exhibited monooriented kinetochores as in the case in YSR13 upon depletion of Dad2. Together, these observations suggest that the conserved arginine residue R126 in the DSS motif plays a critical role in facilitating biorientation of the kinetochores, lacking which cells remain arrested at metaphase. The fact that the mutants expressing ScDad2-R126A or ScDad2-ΔDSS mimic the nature and severity of the phenotype observed upon depletion of Dad2 suggests the DSS region, particularly its R126 residue, plays a significant role in the proper functioning of the Dam1 complex in *S. cerevisiae*.

The conserved arginine residue in the DSS is essential for faithful chromosome segregation in *C. albicans*

To test for functional conservation of the DSS in *C. albicans*, we used the strains ASR02, ASR03 and ASR04 expressing CaDad2-FL, CaDad2-R92A, and CaDad2-ΔDSS respectively from the native genomic locus. Any defect in the structural integrity of the kinetochore caused by the mutations introduced in the DSS is expected to result in the disintegration of the kinetochore ensemble followed by proteasomal degradation of CENPA in *C. albicans* (Thakur and Sanyal 2012). We engineered the strains ASR02 through ASR04 to express Protein-A tagged CENPA to assay for such defects. Immunoblotting revealed comparable levels of CENPA between ASR07

cells expressing CaDad2-FL, and the mutant strains ASR08 and ASR09, expressing CaDad2-R92A and CaDad2-ΔDSS respectively (Figure 3A). Hence, unlike the depletion of Dad2 or other Dam1 complex subunits, the kinetochore integrity is not compromised in the DSS mutants in *C. albicans* (Thakur and Sanyal 2012). The punctate localization signals, typical of a kinetochore protein, as observed in cells expressing the mutant Dad2 (Figure 1G) further supports the fact that neither the deletion of the DSS nor substitution in the conserved arginine residue in the DSS affects the kinetochore assembly in *C. albicans*.

To further understand the growth defects of *dad2* mutants at a lower temperature, we grew these strains overnight at 30°C, reinoculated them to fresh media in duplicates, and allowed them to complete two generations each at 30°C and 18°C, respectively. Analysis of cell cycle progression of strains grown at 30°C revealed a modest increase in the proportion of cells at the G2/M stage when they expressed CaDad2-R92A as in ASR03 or CaDad2-ΔDSS as in ASR04 when compared to the control strain ASR02 that expressed CaDad2-FL (Figure 3B, Figure S2A). The frequency of G2/M arrested cells was further amplified when the DSS mutants were grown at 18°C wherein most of the cells displayed this phenotype (Figure 3B). Given that the kinetochore assembly remained unaffected in the DSS mutants (Figure 1G and 3A), we suspected the moderate increase in cells at G2/M and cold-sensitive phenotype of these mutants to be consequential of aberrant kinetochore-MT interactions.

When cells were collected for flow cytometry analysis, additional aliquots of similarly grown cells were examined to analyze their nuclear segregation patterns in the strains ASR02, ASR03 and ASR04 expressing CaDad2-FL, CaDad2-R92A, and CaDad2-ΔDSS respectively. We observed ~2-fold increase in the frequency of defective nuclear segregation in strains expressing CaDad2-R92A and CaDad2-ΔDSS as compared to cells expressing CaDad2-FL when grown at 30°C (Figure 3C). This frequency further increased to >3-fold when these strains were grown at 18°C (Figure 3C). Each of these strains was engineered to express an SPB marker Tub4-mCherry to study the spindle dynamics and correlate them with the frequency of defective nuclear segregation. In the strains ASR13 and ASR14 expressing CaDad2-R92A and CaDad2-ΔDSS respectively, we observed a significant increase in the frequency of large-budded cells showing short spindles (< 2 µm) as compared to ASR12 that expressed CaDad2-FL at 30°C (Figure 3D). This was further reflected in the reduction in the average spindle length in these mutant strains

(Figure 3E). We were unable to perform this assay at 18°C as the DSS mutants showed an aberrant elongated large-budded phenotype at this temperature, suggesting that epitope-tagged Tub4 could be non-functional in this condition. The increased proportion of cells at metaphase with the spindle length (SPB-SPB distance) of < 2 µm and an unsegregated nuclear mass is suggestive of a delayed anaphase onset in these mutants.

The observed delay in mitotic progression could be due to the inability of these mutants to achieve a bioriented state, as observed in *S. cerevisiae* (Figure 2D). Such defective kinetochore-MT attachments which do not generate tension are detected by sensors like the Aurora B kinase (Ipl1 in yeast) that eventually activate the spindle assembly checkpoint until proper biorientation is achieved. We suspected that the accumulation of cells with metaphase-like spindle in the DSS mutants could also be due to a similar defect. As mentioned above, ASR03 (CaDad2-R92A-GFP) and ASR04 (CaDad2-ΔDSS-GFP) cells were arrested completely at the G2/M stage when grown at 18°C. We selected this condition to score for bypass of the G2/M arrest in the corresponding checkpoint deficient mutants ASR17 (Δ*mad2* CaDad2-R92A-GFP) and ASR18 (Δ*mad2* CaDad2-ΔDSS-GFP) by flow cytometry (Figure S2B). The presence of unbudded cells (2N population) in ASR17 and ASR18 mutants as compared to the G2/M arrested phenotype in ASR03 and ASR04 cells suggested that the DSS mutants were indeed arrested at metaphase. We also analyzed these strains for segregation of the sister kinetochores marked by CaDad2-GFP when grown at 30°C and 18°C (Figure S2C). At both the temperatures tested, the percentage of large-budded cells with unsegregated sister kinetochores in the mother bud (< 2 µm between CaDad2 puncta) was reduced in the checkpoint deficient Dad2 mutants ASR17 and ASR18 as compared to their checkpoint-proficient parent strains, further validating a delay in anaphase onset in these cells.

By comparing the results obtained thus far in *S. cerevisiae* and *C. albicans,* it is evident that the function of the DSS is conserved between these species, with an obvious reduction in the severity of the Dad2 mutant phenotype in *C. albicans*. The Dam1 complex is known to play a critical role in chromosome segregation by strengthening the kinetochore-MT associations, especially in instances where a single MT binds to a chromosome like in *S. cerevisiae* and *C. albicans.* Although the number of MTs binding a chromosome is the same between these species, a single CENPA nucleosome forms the basis of MT attachment in *S. cerevisiae*. On the other hand, one among four CENPA nucleosomes anchors the MTs in *C. albicans*. We speculated that the

presence of additional CENPA nucleosomes confers a degree of tolerance towards mutations in the DSS. To test if this was indeed the case, we resorted to a basidiomycetous yeast *C. neoformans* known to have large regional centromeres harboring 27- 64 kb long CENPA enriched regions (Janbon et al. 2014; Yadav et al. 2018), suggestive of having CENPA nucleosomes in excess of that known in *C. albicans* (Joglekar et al. 2008; Coffman et al. 2011a). Besides, the Dam1 complex subunits have been characterized and shown essential for chromosome segregation in this organism, making it an ideal system to test our hypothesis (Sridhar et al. 2021).

The conserved arginine R102 in CnDad2 is dispensable for mitotic progression in *C. neoformans*

We generated constructs to introduce an alanine substitution mutation in the conserved arginine residue (R102 in CnDad2) as well as for the deletion of the entire DSS region in CnDad2 and express them along with mCherry tagged at the C- terminus in *C. neoformans* (Figure 3F). As a control, another construct to express an unaltered full-length CnDad2 sequence was also generated. Each of these constructs was used to transform the strain CNV108 (expressing GFP-H4) (Kozubowski et al. 2013) to generate CNSD169 (CnDad2-FL-mCherry, GFP-H4), CNSD170 (CnDad2-R102A-mCherry, GFP-H4), and CNSD171 (CnDad2-ΔDSS-mCherry, GFP-H4).

Spot dilution assays performed at routine growth conditions in YPD at 30°C revealed that neither the point mutation R102A nor the deletion of the entire DSS motif of CnDad2 resulted in an obvious growth defect, suggesting that the DSS mutants are viable in *C. neoformans* as well (Figure 3G). We also examined growth inhibitions of these mutants at a lower temperature (14°C) or in the presence of thiabendazole (6 µg/mL), conditions used to test mutants for defective kinetochore-MT associations. We failed to observe any growth defects in the mutant strains CNSD170 and CNSD171 expressing CnDad2-R102A CnDad2-ΔDSS respectively, as compared to CNSD169 cells expressing CnDad2-FL (Figure 3G). To corroborate these observations, we grew each of these strains to log phase at 30°C (Figure 3H). We did not observe a significant increase in the number of large-budded cells in strains expressing wild-type or mutant versions of Dad2 bearing alanine substituted conserved arginine residue in the DSS or deletion of the entire DSS itself (Figure 3H). However, further analysis of nuclear segregation by localization of GFP-tagged histone H4 revealed that the CNSD171 mutant strain expressing the DSS deletion, but not CNSD170 with the point mutation CnDad2-R102A, had a significant increase in the proportion of

large-budded cells with an unsegregated nuclear mass (Figure 3I). This suggested that the arginine residue is conserved but, unlike in *S. cerevisiae* or *C. albicans*, dispensable for viability in *C. neoformans*. However, a small but significant increase in the large bud arrested cells when the entire DSS was deleted, suggested importance of the motif in chromosome segregation in *C. neoformans*.

The wild-type-like behavior of the CnDad2-R102A mutant strain is suggestive of a redundant function of the conserved arginine residue in this species as compared to *S. cerevisiae* or *C. albicans*. Despite a high level of conservation at the amino acid sequence in the DSS, the striking differences in the dependence on this conserved arginine residue for mitotic progression across the evolutionarily diverged species can be attributed to the differences in the centromere length.

Discussion

In this study, we identify an evolutionarily conserved domain, the DSS, at the C-terminus of Dad2 that hosts a highly conserved arginine residue. Our phylogenetic analysis of sequenced genomes across Ascomycota, Basidiomycota, and many species of Mucoromycota, reveals that the arginine residue is positively selected for about 700 million years. Alanine substitution analysis suggests that this arginine residue in the DSS motif is essential for viability and timely mitotic progression in *S. cerevisiae* as the mutant cells arrested at the G2/M stage with a metaphase-like spindle. The presence of monooriented kinetochores in the DSS mutants in *S. cerevisiae* highlights the mechanistic significance of the conserved arginine residue in establishing sister chromatid biorientation in an organism with point centromeres. We observed similar mitotic defects, albeit at a lower frequency, when the corresponding arginine residue was mutated to alanine in Dad2 in *C. albicans* harboring small regional centromeres. A small but significant increase in mitotic defects was observed only upon deletion of the entire DSS in *C. neoformans* that possesses large regional centromeres. The alanine substitution of the conserved arginine in the DSS is neither lethal nor caused a high rate of chromosome missegregation, suggestive of a redundant function conferred by the arginine residue in *C. neoformans*. The diminishing significance of the DSS as the length of centromeric chromatin increases established in this study, tempted us to speculate that larger centromeres may have evolved to develop tolerance to mutations that cause lethality to an organism possessing short point centromeres (Figure 4A).

One of the early mitotic roles of the Dam1 complex is in the establishment and maintenance of sister chromatid biorientation until the SAC is satisfied (Cheeseman et al. 2001a; Janke et al. 2002; Franco et al. 2007; Tanaka et al. 2007). Conditional mutants of Dam1 complex subunits arrest at the large-budded stage with short spindles and an unsegregated nuclear mass (Cheeseman et al. 2001b; Janke et al. 2002; Li et al. 2002). We find a similar phenotype upon alanine substitution of the conserved arginine in the DSS in *S. cerevisiae*. This suggests that the DSS, particularly the conserved arginine R126, could play an essential role in the overall integrity of the Dam1 complex *in vivo*. Some of the known factors that govern the function of the Dam1 complex include (a) its interaction with the MTs and the Ndc80 complex for kinetochore localization (Janke et al. 2002; Li et al. 2002; Wong et al. 2007; Maure et al. 2011; Lampert et al. 2013; Kim et al. 2017), and (b) its ability to oligomerize to a ring-like structure that enables it to sustain its MT association under tension (Miranda et al. 2007; Umbreit et al. 2014; Zelter et al. 2015). Any of these functional dependencies could be disrupted upon alanine substitution of the conserved arginine in the DSS or deletion of the entire DSS itself, making the mutant phenotype similar to the loss of an entire Dam1 complex subunit in *S. cerevisiae*. From the analysis of the conservation of amino acids in the DSS, it is evident that the arginine residue is preferred even over other positively charged amino acids at the 126th position in ScDad2 or the corresponding position in other species. The length of the sidechain of this conserved arginine and the interactions with its neighborhood may be critical for the overall stability or function of the Dam1 complex, apart from its inherent positive charge (Figure S3). Further biochemical characterization of a recombinant mutant Dam1 complex containing mutated versions of Dad2 such as Dad2-R126A or Dad2-ΔDSS will shed light on this aspect. Previous studies on Dam1 suggested that the role of such a coupler to the Ndc80 complex is essential in instances of a single MT binding to a chromosome (Winey et al. 1995; Cheeseman et al. 2001b; Janke et al. 2002; Li et al. 2002; Burrack et al. 2011; Thakur and Sanyal 2011). This also explained the essentiality of the Dam1 complex for viability in both *S. cerevisiae* and *C. albicans* despite having distinct lengths of CENPA chromatin (Burrack et al. 2011; Thakur and Sanyal 2011). Considering this, how does one explain the varied tolerance observed for the alanine substitution of the conserved arginine in the DSS between the two species?

In an organism like *S. cerevisiae*, a single kinetochore module, assembled on 1-2 CENPA nucleosomes, serves as a MT receptor on each chromosome (Joglekar et al. 2006; Furuyama and

Biggins 2007; Cieslinski et al. 2021). Hence, the single critical point of contact between the receptor and a single MT solely determines sister chromatid biorientation and their subsequent segregation. Thus, it is conceivable that mutations that compromise this delicate kinetochore-MT association would not be tolerated in *S. cerevisiae* (Figure 4B). Indeed, several point mutants of subunits of the Dam1 complex have been shown to be lethal (Cheeseman et al. 2001a; Janke et al. 2002). On the other hand, about 4 CENPA nucleosomes are shown to be present on each 3-5 kb long centromeric chromatin in *C. albicans* (Joglekar et al. 2008). Strikingly, the outer kinetochore modules that interface centromeric chromatin and kMTs are sufficient to form only a single MT receptor in a wild-type scenario (Joglekar et al. 2008). Despite binding a single MT as observed in *S. cerevisiae*, the alanine substituted Dad2-R92A mutant in *C. albicans* is viable. We speculated that this apparent discrepancy might be explained if additional kinetochore subunits could be recruited to these 'spare' CENPA nucleosomes in *C. albicans*, serving as receptors that facilitate the binding of multiple MTs to a chromosome when a 'need' arises. Such a failsafe mechanism can ensure proper chromosome segregation even with a weaker mutant kinetochore (Figure 4B). The subset of cells that were unable to recruit excess outer kinetochore subunits may fail to segregate chromosomes, thereby losing viability. Indeed, we observed significantly higher levels of Ndc80 at the kinetochore cluster in the DSS mutants that were able to segregate their chromosomes in post-metaphase cells as compared to the control wild-type cells (Figure 4C). This clearly demonstrates that the survivors in mutant strains expressing mutant versions of Dad2 such as CaDad2-R92A and CaDad2-ΔDSS are primed to recruit multiple MTs to a chromosome.

The fundamental requisites for a cell to operate such a mechanism are the availability of surplus kinetochore subunits and the ability to seed the required number of additional MTs. Overexpression of CENPA in *C. albicans* has been shown to increase the copy number of the outer kinetochore proteins without crossing the wild-type boundaries of centromeric chromatin (Burrack et al. 2011). The enrichment of CENPA itself increases upon overexpression, suggesting that these regional centromeres can indeed accommodate additional CENPA molecules and the other kinetochore subcomplexes it associates with. Even the budding yeast that binds a single MT to its chromosomes can be engineered to seed additional kMTs suggesting that the stoichiometry of the number of kMTs to the number of chromosomes can be dynamic (Nannas et al. 2014). These studies that suggest that neither the required levels of kinetochore proteins nor the number of MTs associates with a kinetochore is limiting in a cell, further supporting our model. The inability of

this failsafe mechanism to tolerate mutations in the DSS in *S. cerevisiae* can be ascribed to their point centromere structure. The size restriction imposed by the point centromere configuration prevents the enrichment of surplus kinetochore proteins at the native centromere, thereby impeding the formation of additional MT attachments.

What would be the consequence of alanine substitution of the conserved arginine in the DSS in an organism with long centromeric chromatin that can support multiple MT binding even in wild-type cells? We addressed this question in *C. neoformans* that possess large regional centromeres with centromeric chromatin ranging between 27 and 64 kb (Yadav et al. 2018). Based on the number of CENPA nucleosomes in a centromere from species like *C. albicans* and *S. pombe* (Joglekar et al. 2008; Coffman et al. 2011b; Rhind et al. 2011), we expect at least 10 CENPA nucleosomes present on each *C. neoformans* centromeres (Figure 4D). Each *S. pombe* centromere containing 10-15 CENPA nucleosomes enriched over a ~10 kb-long centromeric chromatin binds to about 2-3 MTs (Ding et al. 1993). Similarly, ~4 MTs have been shown to associate with centromeres in chicken and fly cells that span more than 30 kb in length (Ribeiro et al. 2009; Ribeiro et al. 2010; Shang et al. 2010). From these studies, we speculate multiple MTs (>2 kMTs) to bind to each chromosome in *C. neoformans* wild-type cells. Since multiple MTs could naturally be associated with each kinetochore, *C. neoformans* cells show better tolerance to mutations in the DSS, in physiological as well as stress conditions like low-temperature growth or in the presence of sub-lethal doses of spindle poisons like thiabendazole.

Our study highlights the progressive loss of essentiality of a conserved arginine residue in Dad2, a Dam1 complex subunit with an increased length of centromeric chromatin. The smallest known centromeres, the point centromeres, are phylogenetically restricted to the Saccharomycotina among the ascomycetes (Guin et al. 2020b). The regional centromere structure with several variations such as unique, repeat-associated, and repetitive is more prevalent in other fungal phyla and metazoans (reviewed in (Guin et al. 2020b; Talbert and Henikoff 2020)). Previously it was hypothesized that large centromeres act as a buffer enabling harmless kinetochore drift across the centromere to prevent functional interference of neighboring essential genes (Fukagawa and Earnshaw 2014). In this study, we uncover another potential advantage associated with regional centromeres, more specifically surplus CENPA nucleosomes, in tolerating conditions sub-optimal for chromosome segregation. Although the presence of

peripheral CENPA as a cloud is conserved across the point and regional centromere structures (Burrack et al. 2011; Coffman et al. 2011b; Lawrimore et al. 2011; Scott and Bloom 2014; Wisniewski et al. 2014; Cieslinski et al. 2021), the opportunity to nucleate a mature kinetochore with the ability to bind to a MT, is only possible in regional centromeres that can accommodate additional CENPA nucleosomes. This adaptive edge provided by regional centromeres in enabling compensatory mechanisms may explain their recurring presence across Eukaryota (Figure 4E, Table S1).

Materials and methods

Media and growth conditions

S. cerevisiae, C. albicans, and *C. neoformans* strains used in this study were grown in YPD (2% dextrose, 2% peptone, 1% yeast extract supplemented with 0.01% adenine) and incubated at 30°C at 180 rpm. Conditional expression strains in *S. cerevisiae* were propagated in galactose media (YPG, 2% galactose, 0.3% raffinose, 2% peptone, 1% yeast extract) unless repression in YPD is mentioned. Transformation of *S. cerevisiae* and *C. albicans* were performed by standard lithium acetate-PEG method (Geitz and Schiestel (2007), Sanyal and Carbon (2002)). Biolistic transformation method was used for *C. neoformans* strains (Davidson et al., 2000). Selection of transformants was based on prototrophy for the metabolic markers used. In case of antibiotic marker NAT, selection was done in media supplemented with 100 µg/mL nourseothricin (ClonNAT; CAS 96736-11-7, Werner Bioagents, Jena, Germany). For cold sensitivity assays, the growth temperature was reduced to 18°C for *C. albicans* and 14°C for *C. neoformans.* For thiabendazole sensitivity assay, the growth media was supplemented with indicated concentration of Thiabendazole (Sigma, 10mg/mL stock in dimethyl formamide).

Strains and plasmids

The list of all the strains, plasmids, and primers used are provided in Tables S2, S3 and S4 respectively. The construction of each of them is detailed below.

Construction of *S. cerevisiae* strains

Construction of vectors to express Dad2-GFP (wildtype, mutated, or truncated form) in pRS313

To express GFP tagged ScDad2 from pRS313 (CEN/ARS/HIS1 plasmid), sequences coding for GFP along with terminator sequences of ScACT1 was amplified using primer pair ScGFP-F/ScGFP-R and cloned as a BamHI-ClaI fragment into pRS313 resulting in pRS313G. This plasmid was subsequently used to clone Dad2 with/without mutations. For cloning ScDad2-FL, a fragment containing ScDAD2pr-

DAD2 ORF was amplified from the genomic DNA of BY4741 strain with primers SR282/SR290 and cloned in frame with GFP as a SacII-BamHI fragment into pRS313G. The resulting plasmid was named pSR01. Since the DSS in ScDad2 is located near the stop codon, any desired mutation was incorporated in the reverse primer used to amplify Dad2. In this way, ScDad2-R126A, ScDad2- R128A, and ScDad2ΔDSS were amplified with primer pairs SR289/Sc126A-R, SR289/Sc128A-R, and SR289/ScΔDSS-R respectively, and cloned into the SacII-BamHI sites of pRS313G. The resulting plasmids were named pSR02 through pSR04. Each of these constructs was confirmed by Sanger sequencing using SR282.

Construction of strains YSR01 through YSR05

A previously reported conditional mutant of ScDad2 (CJY077: *MATa Δdad2::KanMX6 ura3-52 lys2-801 ade2-101 trp1Δ63 leu2Δ1::pCJ055(dad2^{ts}, LEU2) his3Δ200*) was used as the parent strain. The plasmids pRS313G, pSR01- pSR04 were used to transform the CJY077 strain by the standard lithium acetate method to generate strains YSR01 through YSR05 respectively. Transformants were selected on CM-leu-his media upon incubation at 28˚C. Selected colonies from the transformation plate were streaked again on CM-leu-his media for single colonies and used for subsequent experiments.

Construction of strains YSR06 through YSR12

The strain BY4741 was engineered to express Spc42 with mCherry tag at the C- terminus resulting in YSR06. The cassette was amplified from the plasmid pAW8-mCherry using the primer pair S42F/S42R. A Dad2 protection plasmid was constructed as follows. The Sc*DAD2* gene with its promoter and terminator was amplified using the primer pair ScDad2Pr F/ScDad2R and cloned as a SacII/SacI fragment into pRS316 (CEN/ARS/URA) resulting in the plasmid pSR05. The strain YSR06 was transformed with the plasmid pSR05 by the standard lithium acetate method to generate strain YSR07. The transformants were selected on CM-ura media upon incubation at 30°C.

YSR07 cells grown on CM-URA media were then transformed with a cassette to delete DAD2 ORF with a *LEU* marker. The cassette was amplified from the plasmid pUG73 using the primer pair ScDad2delF/ScDad2delR. Since the deletion cassette can delete DAD2 from either the native locus or from the plasmid, the desired transformants where the deletion occurred on the genomic DAD2 locus were selected by their inability to grow on media containing 5'FOA. This strain was named YSR08 and was further confirmed by PCR using the primer pair ScDad2F/Leu2R. Strains YSR09- YSR12 were subsequently generated by independently transforming YSR08 cells with plasmids pSR01-pSR04. The transformants were selected on CM-ura-his media upon incubation at 30˚C. The strains YSR09 through YSR12 were subsequently maintained in this media unless stated otherwise.

Construction of strains YSR13 through YSR17

A cassette to replace the native DAD2 promoter with the *GAL*$_{1\text{-}10}$ promoter was amplified with the primer pairs GalDad2FP/GalDad2RP using pYM-N25 as the template. The PCR product was used to transform the strain SBY12503 to obtain the conditional mutant strain YSR13. The transformants were selected on YPDU plates supplemented with 100 µg/mL norseothricin upon incubation at 30°C.

For integrating ScDad2-FL, the ORF containing fragment was amplified using the primers Dad2pr-SacII-F/ Dad2pr-SacI-R. A reintegration cassette was generated by cloning the *DAD2* ORF along with the promoter in SacII/SacI sites into pUG73 resulting in pSR06. To introduce mutations corresponding to ScDad2-R126A, ScDad2-R128A, and ScDad2-ΔDSS, the ORF containing fragments were constructed by overlap PCR (see list of primers). Each of these fragments were independtly cloned as SacII-SacI fragment into pUG73 resulting in plasmids pSR07 (ScDad2-R126A in pUG73), pSR08 (ScDad2-R128A in pUG73) and pSR09 (ScDad2-ΔDSS in pUG73).

Each of these plasmids pSR06-pSR09 was linearized by digestion with SpeI and then used to transform the conditional mutant strain YSR13 to obtain reintegrants YSR14-YSR17 that respectively express ScDad2-FL, ScDad2-R126A, ScDad2-R128A, and ScDad2-ΔDSS from the DAD2 promoter from the native *DAD2* locus. The transformants were selected on CM(Gal)-leu media upon incubation at 30°C.

Construction of *C. albicans* strains

Construction of strains J108A and J108B

A plasmid pBS-RN was constructed by amplifying the *RPS1* locus using the primer pair RP10F/RP10R and cloned as a NotI fragment into the pBS-NAT plasmid. A previously reported plasmid pDad2-TAP was used as a template to amplify wild-type full length *DAD2* along with its promoter and a C-terminal TAP tag using the primer pair AD02/AD03. The amplicon was cloned as a SalI fragment into pBS-RN resulting in the plasmid pRN-Dad2-FL. The DSS deleted version was generated by overlap PCR strategy using the primer pairs AD02/Dad2delR and Dad2delF/AD03. The overlap product was cloned as a SalI fragment into pBS-RN to obtain the plasmid pRN-Dad2-ΔDSS. Both pRN-Dad2-FL and pRN-Dad2-ΔDSS were used to transform the conditional *dad2* mutant J108 after linearization with StuI. The transformants were selected on YP-Succinate media supplemented with 200 µg/mL NAT.

Construction of strains ASR01 through ASR04

A previously reported plasmid pDad2Δ3 (*CaDAD2* deletion with a *HIS1* marker) was used to transform SN148 after digestion with SacI-KpnI. The resulting heterozygous mutant of *DAD2* was named ASR01. The vectors to incorporate desired mutations in the remaining *DAD2* allele were constructed as follows.

Sequences 537 bp downstream of the *DAD2* ORF was amplified using the primer pair Dad2DS-F/Dad2DS-R and cloned as a XhoI/KpnI fragment into pBS-GFP-Ura plasmid. The resulting plasmid was named pSR10 and was used to clone the other homology region containing *DAD2* ORF with desired mutations. In this regard, mutant version of *DAD2* were generated by overlap PCR method as described earlier and the product was cloned into pBS-RN resulting in plasmids pRN-92(for CaDad2-R92A). Along with pRN-Dad2-FL and pRN-Dad2-ΔDSS these plasmids served as intermediate vectors from which *CaDAD2* ORF with the corresponding mutation was amplified using the primer pair Dad2FP/Dad2GFP-RP. Each of these fragments were cloned as a SacII/SpeI fragment into pSR10 resulting in plasmids pSR11 (CaDad2-FL), pSR12 (CaDad2-R92A), and pSR15 (CaDad2-ΔDSS). These plasmids were then used to transform ASR01 after digestion with SacII-KpnI to result in strains ASR02 throughASR04. The transformants were selected in CM-uri media. The presence of desired mutations was confirmed by Sanger sequencing using the primer Dad2cFP.

Construction of strains ASR07 through ASR09

To tag CENP-A with a TAP tag, a previously reported plasmid pCse4TAP-Leu *(Varshney and Sanyal, 2019)*) was linearized with XhoI and used the transform strains ASR02 through ASR04 to obtain the strains ASR07 through ASR09. The transformants were selected on CM-leu plates. Expression of the fusion protein was confirmed by immunoblotting.

Construction of strains ASR12 through ASR14

A plasmid to tag Tub4 with mCherry was generated as follows. The 3' part of the *TUB4* gene was released from a previously reported plasmid pTub4GFP-Ura as a SacII/SpeI fragment and cloned into pDam1-mCherryNAT at these sites, replacing *DAM1* with *TUB4*. The resulting plasmid pTub4-mCherryNAT was linearized by XbaI digestion and used to transform the strains ASR02-04 to obtain ASR12 through ASR14. The transformants were selected on YPD plates supplemented with 100 µg/mL NAT. Transformants were confirmed by fluorescence microscopy.

Construction of ASR17 and ASR18

One allele of *MAD2* in ASR03 (CaDad2-R92A) and ASR04 (CaDad2-ΔDSS) was deleted by transformation with the plasmid pMad2-2 (Thakur and Sanyal, 2011) after digestion by SacII-XhoI. The resulting heterozygous *MAD2* mutants were named ASR03M and ASR04M. The transformants were

selected on CM-leu plates. The remaining allele of *MAD2* in ASR03M and ASR04M were deleted by transformation with the plasmid pMad2-3 after digestion with BamHI-XhoI. The resulting *mad2* mutants from ASR03M and ASR04M were named ASR17 and ASR18 respectively. The transformants were selected on CM-leu-arg plates. The strains were confirmed by PCR using primer pairs Mad2-1/Mad2-2 and NV228/NV229.

Construction of strains ASR19 through ASR21

To tag Ndc80 with mCherry, a previously reported plasmid pNdc80-mChARG *(Varshney and Sanyal, 2019)*) was linearized with XhoI and used the transform strains ASR02 through ASR04 to obtain the strains ASR19 through ASR21. The transformants were selected on CM-arg plates. Expression of the fusion protein was confirmed by microscopy.

Construction of *C. neoformans* strains

Construction of strains CNSD169 through CNSD171

A 743 bp fragment that includes Dad2 promoter and the ORF was amplified by overlap PCR using the primer pairs SD118/SD119 and SD120/VYP152 to introduce the mutation R102A in CnDad2. By a similar overlap PCR based strategy, DSS deleted version of CnDad2 was also amplified. A second fragment containing mCherry tag along with a Neomycin marker was amplified from pLK25 using the primer pairs VYP153/VYP154. The homology region corresponding to the DAD2-3'UTR was amplified using VYP155/VYP156. These three fragments were subsequently fused by overlap PCR using the primer pairs SD118/VYP156 and used to transform the strain CNV108 by biolistic method. For the control strain, the same overlap PCR strategy was used with the first homology region amplified without any mutation using primer pairs SD118/VYP152. Transformants were selected by resistance to Neomycin and were further confirmed by PCR and Sanger sequencing.

Identification of DSS

The HMM file for the Dad2 domain (PF08654) was downloaded from the Pfam database page for this domain. This model was used as the query to perform a HMMsearch (hmmsearch search | HMMER (ebi.ac.uk)) routinely used to search for a HMM profile against a protein sequence database. The search was targeted against fungal genomes using the option 'Ensembl Genomes Fungi'. The E-value cutoff for the search was 0.01 by default. The first round of HMM search resulted in 912 hits from all the major fungal subphyla (Supplementary table S5, Sheet- Hits_Ensembl Fungi). The hits were manually curated to remove duplicate entries of any given species for which multiple genome sequences were available. In addition to this, hits from 9 species that were unusually long were also removed for subsequent analysis

to avoid alignment artifacts (Supplementary table S5, Sheet- long hits). This resulted in a final pool of 466 hits from which a multiple sequence alignment was generated using MAFFT. Apart from the known Dad2 domain at the N- terminus, the alignment revealed a second conserved domain Dad2 centered around a highly conserved arginine. This 10aa-long domain was named DSS. The amino acid logo indicating the consensus sequence of DSS (in Figure 1A) was generated with this multiple sequence alignment using Weblogo tool (WebLogo - Create Sequence Logos (berkeley.edu)).

Flow cytometry

Overnight grown cultures of *S. cerevisiae* or *C. albicans* were subcultured to0.2 OD_{600} in desired media/ growth condition as described for the experiment. Cells were harvested at various time intervals post-inoculation. Harvested samples were fixed by dropwise addition of ice-cold 70% ethanol, followed by RNAse treatment and propidium iodide (PI) staining as described before (Sanyal and Carbon, PNAS 2002). Stained cells were diluted to the desired cell density in 1x PBS and analyzed (30, 000 cells) by flow cytometry (FACSAria III, BD Biosciences) at a rate of 500-2000 events/s. The output was analyzed using the FLOWJO software. The 561-nm laser was used to excite PI and 610/20 filter to detect its emission signals.

Fluorescence microscopy and analysis

Cells were grown in media and growth conditions as described for each experiment. Prior to imaging, the cells were washed thoroughly with sterile water twice and resuspended in sterile water to achieve optimum cell density for imaging. The cells were imaged in Zeiss Axio observer equipped with Colibri 7 as the LED light source, 100x Plan Apochromat 1.4 NA objective, and PCO edge 4.2 sCMOS camera. Z sections were obtained at an interval of 300 nm. All the images were displayed after the maximum intensity projection using ImageJ. For visualizing nuclear mass, *S. cerevisiae* and *C. albicans* cells were stained with Hoechst (50 ng/mL) prior to imaging. GFP and mCherry fluorescence were acquired using the filter set 92 HE (excitation 455–483 nm and emission 501–547 nm for GFP, and excitation 583–600 nm and emission 617–758 nm for mCherry).

Western blotting

Protein lysates for western blot were prepared by the TCA method. From overnight grown cultures, 3OD_{600} equivalent cells were harvested, washed, and resuspended in 400 µL of 12.5 % ice cold TCA solution. The suspension was vortexed briefly and stored at - 20°C for 12 h. The suspension was thawed on ice, pelleted at 14000 rpm for 10 min and washed twice with 350 µL of 80 % Acetone (ice cold). The washed pellets were air dried completely and resuspended in desired volume of lysis buffer (0.1N

NaOH+1% SDS). Rabbit anti-Protein A antibody (P3775, Sigma) and the HRP conjugated Goat anti-Rabbit secondary antibody, both were used at 1:5000 dilution in 2.5 % Skim Milk powder in 1XPBS. The blots were developed using chemiluminescent substrate (BioRad) and imaged using Chemidoc system (BioRad)

Statistical analysis

All graphs were generated and analyzed using Graphpad prism (v8). One-way ANOVA or paired t-test with Welsch's correction was used based on the sample size to test for the statistical significance of acquired results using a *p*-value cut off of 0.05.

Competing interest statement

The authors declare no competing interests.

Acknowledgment

We thank S. Biggins (Fred Hutchinson Cancer Research Center, Seattle) for sharing strains and N. Nala for providing technical support in using the in-house flow cytometry facility at JNCASR. We also thank T.K. Manna and Renjith MR (IISER, Thiruvananthapuram), H. Balaram and A. Bellur (JNCASR, Bangalore), and K.V.R. Chary (IISER, Berhampur) for useful discussions and feedback. SRS is a research associate supported by intramural funding by JNCASR. SP is a senior research fellow supported by the graduate research fellowship from JNCASR. AAJ is supported by the Wellcome Trust through a Senior Research Fellowship (202811). KS is a JC Bose National Fellow (JCB/2020/000021) of SERB. AD was a research associate supported by JNCASR. KS acknowledges financial support from DBT, SERB, and intramural funding from JNCASR.

Author contributions

KS conceived the idea, planned the study, secured funding, analyzed data, and supervised the study. SRS performed Dad2 sequence analysis, and all experiments related to *S. cerevisiae* and *C. albicans* and analyzed data. SP performed experiments on *C. neoformans*. AD performed initial experiments to identify and understand the DSS function in *C. albicans* and provided insights from preliminary biochemical studies. AAJ analyzed the available Dam1 complex structure and

identified potential contacts between the DSS and other subunits of the complex. SRS and KS wrote the manuscript with input from all coauthors.

References

Ananiev EV, Phillips RL, Rines HW. 1998. Chromosome-specific molecular organization of maize (Zea mays L.) centromeric regions. *Proc Natl Acad Sci U S A* **95**: 13073-13078.

Berbee ML, James TY, Strullu-Derrien C. 2017. Early Diverging Fungi: Diversity and Impact at the Dawn of Terrestrial Life. *Annu Rev Microbiol* **71**: 41-60.

Brooks CF, Francia ME, Gissot M, Croken MM, Kim K, Striepen B. 2011. Toxoplasma gondii sequesters centromeres to a specific nuclear region throughout the cell cycle. *Proc Natl Acad Sci U S A* **108**: 3767-3772.

Burrack LS, Applen SE, Berman J. 2011. The requirement for the Dam1 complex is dependent upon the number of kinetochore proteins and microtubules. *Curr Biol* **21**: 889-896.

Cambareri EB, Aisner R, Carbon J. 1998. Structure of the chromosome VII centromere region in Neurospora crassa: degenerate transposons and simple repeats. *Mol Cell Biol* **18**: 5465-5477.

Chatterjee G, Sankaranarayanan SR, Guin K, Thattikota Y, Padmanabhan S, Siddharthan R, Sanyal K. 2016. Repeat-associated fission yeast-like regional centromeres in the ascomycetous budding yeast *Candida tropicalis*. *PLoS Genet* **12**: e1005839.

Cheeseman IM. 2014. The kinetochore. *Cold Spring Harb Perspect Biol* **6**: a015826.

Cheeseman IM, Brew C, Wolyniak M, Desai A, Anderson S, Muster N, Yates JR, Huffaker TC, Drubin DG, Barnes G. 2001a. Implication of a novel multiprotein Dam1p complex in outer kinetochore function. *J Cell Biol* **155**: 1137-1145.

Cheeseman IM, Enquist-Newman M, Muller-Reichert T, Drubin DG, Barnes G. 2001b. Mitotic spindle integrity and kinetochore function linked by the Duo1p/Dam1p complex. *J Cell Biol* **152**: 197-212.

Cieslinski K, Wu Y-L, Nechyporenko L, Hörner SJ, Conti D, Ries J. 2021. Nanoscale structural organization and stoichiometry of the budding yeast kinetochore. *bioRxiv*: 2021.2012.2001.469648.

Coffman VC, Wu P, Parthun MR, Wu J-Q. 2011a. CENP-A exceeds microtubule attachment sites in centromere clusters of both budding and fission yeast. *Journal of Cell Biology* **195**: 563-572.

Coffman VC, Wu P, Parthun MR, Wu JQ. 2011b. CENP-A exceeds microtubule attachment sites in centromere clusters of both budding and fission yeast. *J Cell Biol* **195**: 563-572.

Coughlan AY, Hanson SJ, Byrne KP, Wolfe KH. 2016. Centromeres of the yeast *Komagataella phaffii (Pichia pastoris)* have a simple inverted-repeat structure. *Genome Biol Evol* **8**: 2482-2492.

Coughlan AY, Wolfe KH. 2019. The reported point centromeres of Scheffersomyces stipitis are retrotransposon long terminal repeats. *Yeast* **36**: 275-283.

Dhatchinamoorthy K, Shivaraju M, Lange JJ, Rubinstein B, Unruh JR, Slaughter BD, Gerton JL. 2017. Structural plasticity of the living kinetochore. *J Cell Biol* **216**: 3551-3570.

Dhatchinamoorthy K, Unruh JR, Lange JJ, Levy M, Slaughter BD, Gerton JL. 2019. The stoichiometry of the outer kinetochore is modulated by microtubule-proximal regulatory factors. *J Cell Biol* **218**: 2124-2135.

Dimitrova YN, Jenni S, Valverde R, Khin Y, Harrison SC. 2016. Structure of the MIND Complex Defines a Regulatory Focus for Yeast Kinetochore Assembly. *Cell* **167**: 1014-1027 e1012.

Diner RE, Noddings CM, Lian NC, Kang AK, McQuaid JB, Jablanovic J, Espinoza JL, Nguyen NA, Anzelmatti MA, Jr., Jansson J et al. 2017. Diatom centromeres suggest a mechanism for nuclear DNA acquisition. *Proc Natl Acad Sci U S A* **114**: 6015-6024.

Ding R, McDonald KL, McIntosh JR. 1993. Three-dimensional reconstruction and analysis of mitotic spindles from the yeast, Schizosaccharomyces pombe. *J Cell Biol* **120**: 141-151.

Echeverry MC, Bot C, Obado SO, Taylor MC, Kelly JM. 2012. Centromere-associated repeat arrays on Trypanosoma brucei chromosomes are much more extensive than predicted. *BMC Genomics* **13**: 29.

Enquist-Newman M, Cheeseman IM, Van Goor D, Drubin DG, Meluh PB, Barnes G. 2001. Dad1p, third component of the Duo1p/Dam1p complex involved in kinetochore function and mitotic spindle integrity. *Mol Biol Cell* **12**: 2601-2613.

Fang Y, Coelho MA, Shu H, Schotanus K, Thimmappa BC, Yadav V, Chen H, Malc EP, Wang J, Mieczkowski PA et al. 2020. Long transposon-rich centromeres in an oomycete reveal divergence of centromere features in Stramenopila-Alveolata-Rhizaria lineages. *PLoS Genet* **16**: e1008646.

Fishel B, Amstutz H, Baum M, Carbon J, Clarke L. 1988. Structural organization and functional analysis of centromeric DNA in the fission yeast Schizosaccharomyces pombe. *Mol Cell Biol* **8**: 754-763.

Fitzgerald-Hayes M, Clarke L, Carbon J. 1982. Nucleotide sequence comparisons and functional analysis of yeast centromere DNAs. *Cell* **29**: 235-244.

Fournier P, Abbas A, Chasles M, Kudla B, Ogrydziak DM, Yaver D, Xuan JW, Peito A, Ribet AM, Feynerol C et al. 1993. Colocalization of centromeric and replicative functions on autonomously replicating sequences isolated from the yeast Yarrowia lipolytica. *Proc Natl Acad Sci U S A* **90**: 4912-4916.

Franco A, Meadows JC, Millar JB. 2007. The Dam1/DASH complex is required for the retrieval of unclustered kinetochores in fission yeast. *J Cell Sci* **120**: 3345-3351.

Fukagawa T, Earnshaw WC. 2014. The centromere: chromatin foundation for the kinetochore machinery. *Dev Cell* **30**: 496-508.

Furuyama S, Biggins S. 2007. Centromere identity is specified by a single centromeric nucleosome in budding yeast. *Proc Natl Acad Sci U S A* **104**: 14706-14711.

Glockner G, Heidel AJ. 2009. Centromere sequence and dynamics in Dictyostelium discoideum. *Nucleic Acids Res* **37**: 1809-1816.

Gong Z, Wu Y, Koblizkova A, Torres GA, Wang K, Iovene M, Neumann P, Zhang W, Novak P, Buell CR et al. 2012. Repeatless and repeat-based centromeres in potato: implications for centromere evolution. *Plant Cell* **24**: 3559-3574.

Gordon JL, Byrne KP, Wolfe KH. 2011. Mechanisms of chromosome number evolution in yeast. *PLoS Genet* **7**: e1002190.

Guin K, Chen Y, Mishra R, Muzaki SRB, Thimmappa BC, O'Brien CE, Butler G, Sanyal A, Sanyal K. 2020a. Spatial inter-centromeric interactions facilitated the emergence of evolutionary new centromeres. *Elife* **9**.

Guin K, Sreekumar L, Sanyal K. 2020b. Implications of the Evolutionary Trajectory of Centromeres in the Fungal Kingdom. *Annu Rev Microbiol* **74**: 835-853.

Harrison GE, Heslop-Harrison JS. 1995. Centromeric repetitive DNA sequences in the genus Brassica. *Theor Appl Genet* **90**: 157-165.

Hofmann C, Cheeseman IM, Goode BL, McDonald KL, Barnes G, Drubin DG. 1998. Saccharomyces cerevisiae Duo1p and Dam1p, novel proteins involved in mitotic spindle function. *J Cell Biol* **143**: 1029-1040.

Hornung P, Troc P, Malvezzi F, Maier M, Demianova Z, Zimniak T, Litos G, Lampert F, Schleiffer A, Brunner M et al. 2014. A cooperative mechanism drives budding yeast kinetochore assembly downstream of CENP-A. *J Cell Biol* **206**: 509-524.

Janbon G, Ormerod KL, Paulet D, Byrnes EJ, 3rd, Yadav V, Chatterjee G, Mullapudi N, Hon CC, Billmyre RB, Brunel F et al. 2014. Analysis of the genome and transcriptome of Cryptococcus neoformans var. grubii reveals complex RNA expression and microevolution leading to virulence attenuation. *PLoS Genet* **10**: e1004261.

Janke C, Ortiz J, Tanaka TU, Lechner J, Schiebel E. 2002. Four new subunits of the Dam1-Duo1 complex reveal novel functions in sister kinetochore biorientation. *EMBO J* **21**: 181-193.

Jenni S, Harrison SC. 2018. Structure of the DASH/Dam1 complex shows its role at the yeast kinetochore-microtubule interface. *Science* **360**: 552-558.

Jiang J, Nasuda S, Dong F, Scherrer CW, Woo SS, Wing RA, Gill BS, Ward DC. 1996. A conserved repetitive DNA element located in the centromeres of cereal chromosomes. *Proc Natl Acad Sci U S A* **93**: 14210-14213.

Joglekar AP, Bouck D, Finley K, Liu X, Wan Y, Berman J, He X, Salmon ED, Bloom KS. 2008. Molecular architecture of the kinetochore-microtubule attachment site is conserved between point and regional centromeres. *J Cell Biol* **181**: 587-594.

Joglekar AP, Bouck DC, Molk JN, Bloom KS, Salmon ED. 2006. Molecular architecture of a kinetochore-microtubule attachment site. *Nat Cell Biol* **8**: 581-585.

Kanesaki Y, Imamura S, Matsuzaki M, Tanaka K. 2015. Identification of centromere regions in chromosomes of a unicellular red alga, Cyanidioschyzon merolae. *FEBS Lett* **589**: 1219-1224.

Kapoor S, Zhu L, Froyd C, Liu T, Rusche LN. 2015. Regional centromeres in the yeast *Candida lusitaniae* lack pericentromeric heterochromatin. *Proc Natl Acad Sci U S A* **112**: 12139-12144.

Kelly JM, McRobert L, Baker DA. 2006. Evidence on the chromosomal location of centromeric DNA in Plasmodium falciparum from etoposide-mediated topoisomerase-II cleavage. *Proc Natl Acad Sci U S A* **103**: 6706-6711.

Kim JO, Zelter A, Umbreit NT, Bollozos A, Riffle M, Johnson R, MacCoss MJ, Asbury CL, Davis TN. 2017. The Ndc80 complex bridges two Dam1 complex rings. *Elife* **6**.

Kipling D, Ackford HE, Taylor BA, Cooke HJ. 1991. Mouse minor satellite DNA genetically maps to the centromere and is physically linked to the proximal telomere. *Genomics* **11**: 235-241.

Kishii M, Nagaki K, Tsujimoto H. 2001. A tandem repetitive sequence located in the centromeric region of common wheat (Triticum aestivum) chromosomes. *Chromosome Res* **9**: 417-428.

Kobayashi N, Suzuki Y, Schoenfeld LW, Muller CA, Nieduszynski C, Wolfe KH, Tanaka TU. 2015. Discovery of an unconventional centromere in budding yeast redefines evolution of point centromeres. *Curr Biol* **25**: 2026-2033.

780 Kozubowski L, Yadav V, Chatterjee G, Sridhar S, Yamaguchi M, Kawamoto S, Bose I, Heitman J, Sanyal K. 2013.
781 Ordered kinetochore assembly in the human-pathogenic basidiomycetous yeast *Cryptococcus neoformans*. *mBio* **4**:
782 e00614-00613.

783 Kunze G, Gaillardin C, Czernicka M, Durrens P, Martin T, Boer E, Gabaldon T, Cruz JA, Talla E, Marck C et al.
784 2014. The complete genome of Blastobotrys (Arxula) adeninivorans LS3 - a yeast of biotechnological interest.
785 *Biotechnol Biofuels* **7**: 66.

786 Lampert F, Hornung P, Westermann S. 2010. The Dam1 complex confers microtubule plus end-tracking activity to
787 the Ndc80 kinetochore complex. *J Cell Biol* **189**: 641-649.

788 Lampert F, Mieck C, Alushin GM, Nogales E, Westermann S. 2013. Molecular requirements for the formation of a
789 kinetochore-microtubule interface by Dam1 and Ndc80 complexes. *J Cell Biol* **200**: 21-30.

790 Lawrimore J, Bloom KS, Salmon ED. 2011. Point centromeres contain more than a single centromere-specific Cse4
791 (CENP-A) nucleosome. *J Cell Biol* **195**: 573-582.

792 Li Y, Bachant J, Alcasabas AA, Wang Y, Qin J, Elledge SJ. 2002. The mitotic spindle is required for loading of the
793 DASH complex onto the kinetochore. *Genes Dev* **16**: 183-197.

794 Liu X, McLeod I, Anderson S, Yates JR, 3rd, He X. 2005. Molecular analysis of kinetochore architecture in fission
795 yeast. *EMBO J* **24**: 2919-2930.

796 Lo AW, Craig JM, Saffery R, Kalitsis P, Irvine DV, Earle E, Magliano DJ, Choo KH. 2001. A 330 kb CENP-A
797 binding domain and altered replication timing at a human neocentromere. *EMBO J* **20**: 2087-2096.

798 Maluszynska J, Heslop-Harrison JS. 1991. Localization of tandemly repeated DMA sequences in Arabidopsis
799 thaliana. *The Plant Journal* **1**: 159-166.

800 Malvezzi F, Litos G, Schleiffer A, Heuck A, Mechtler K, Clausen T, Westermann S. 2013. A structural basis for
801 kinetochore recruitment of the Ndc80 complex via two distinct centromere receptors. *EMBO J* **32**: 409-423.

802 Marie-Nelly H, Marbouty M, Cournac A, Liti G, Fischer G, Zimmer C, Koszul R. 2014. Filling annotation gaps in
803 yeast genomes using genome-wide contact maps. *Bioinformatics* **30**: 2105-2113.

804 Maure JF, Komoto S, Oku Y, Mino A, Pasqualato S, Natsume K, Clayton L, Musacchio A, Tanaka TU. 2011. The
805 Ndc80 loop region facilitates formation of kinetochore attachment to the dynamic microtubule plus end. *Curr Biol*
806 **21**: 207-213.

807 Milks KJ, Moree B, Straight AF. 2009. Dissection of CENP-C-directed centromere and kinetochore assembly. *Mol*
808 *Biol Cell* **20**: 4246-4255.

809 Miranda JJ, King DS, Harrison SC. 2007. Protein arms in the kinetochore-microtubule interface of the yeast DASH
810 complex. *Mol Biol Cell* **18**: 2503-2510.

811 Musacchio A, Desai A. 2017. A molecular view of kinetochore assembly and function. *Biology (Basel)* **6**: 5-54.

812 Nakaseko Y, Adachi Y, Funahashi S, Niwa O, Yanagida M. 1986. Chromosome walking shows a highly
813 homologous repetitive sequence present in all the centromere regions of fission yeast. *EMBO J* **5**: 1011-1021.

814 Nannas NJ, O'Toole ET, Winey M, Murray AW. 2014. Chromosomal attachments set length and microtubule
815 number in the Saccharomyces cerevisiae mitotic spindle. *Mol Biol Cell* **25**: 4034-4048.

816 Narayanan A, Vadnala RN, Ganguly P, Selvakumar P, Rudramurthy SM, Prasad R, Chakrabarti A, Siddharthan R,
817 Sanyal K. 2021. Functional and Comparative Analysis of Centromeres Reveals Clade-Specific Genome
818 Rearrangements in Candida auris and a Chromosome Number Change in Related Species. *mBio* **12**.

819 Navarro-Mendoza MI, Perez-Arques C, Panchal S, Nicolas FE, Mondo SJ, Ganguly P, Pangilinan J, Grigoriev IV,
820 Heitman J, Sanyal K et al. 2019. Early diverging fungus *Mucor circinelloides* lacks centromeric histone CENP-A
821 and displays a mosaic of point and regional centromeres. *Curr Biol* **22**: 3791-3802.

822 Nergadze SG, Piras FM, Gamba R, Corbo M, Cerutti F, McCarter JGW, Cappelletti E, Gozzo F, Harman RM,
823 Antczak DF et al. 2018. Birth, evolution, and transmission of satellite-free mammalian centromeric domains.
824 *Genome Res* **28**: 789-799.

825 Obado SO, Bot C, Nilsson D, Andersson B, Kelly JM. 2007. Repetitive DNA is associated with centromeric
826 domains in Trypanosoma brucei but not Trypanosoma cruzi. *Genome Biol* **8**: R37.

827 Ola M, O'Brien CE, Coughlan AY, Ma Q, Donovan PD, Wolfe KH, Butler G. 2020. Polymorphic centromere
828 locations in the pathogenic yeast Candida parapsilosis. *Genome Res* **30**: 684-696.

829 Padmanabhan S, Thakur J, Siddharthan R, Sanyal K. 2008. Rapid evolution of Cse4p-rich centromeric DNA
830 sequences in closely related pathogenic yeasts, *Candida albicans* and *Candida dubliniensis*. *Proc Natl Acad Sci U S*
831 *A* **105**: 19797-19802.

832 Ravin NV, Eldarov MA, Kadnikov VV, Beletsky AV, Schneider J, Mardanova ES, Smekalova EM, Zvereva MI,
833 Dontsova OA, Mardanov AV et al. 2013. Genome sequence and analysis of methylotrophic yeast Hansenula
834 polymorpha DL1. *BMC Genomics* **14**: 837.

835 Rhind N, Chen Z, Yassour M, Thompson DA, Haas BJ, Habib N, Wapinski I, Roy S, Lin MF, Heiman DI et al.
836 2011. Comparative functional genomics of the fission yeasts. *Science* **332**: 930-936.

837 Ribeiro SA, Gatlin JC, Dong Y, Joglekar A, Cameron L, Hudson DF, Farr CJ, McEwen BF, Salmon ED, Earnshaw
838 WC et al. 2009. Condensin regulates the stiffness of vertebrate centromeres. *Mol Biol Cell* **20**: 2371-2380.

839 Ribeiro SA, Vagnarelli P, Dong Y, Hori T, McEwen BF, Fukagawa T, Flors C, Earnshaw WC. 2010. A super-
840 resolution map of the vertebrate kinetochore. *Proc Natl Acad Sci U S A* **107**: 10484-10489.

841 Sankaranarayanan SR, Ianiri G, Coelho MA, Reza MH, Thimmappa BC, Ganguly P, Vadnala RN, Sun S,
842 Siddharthan R, Tellgren-Roth C et al. 2020. Loss of centromere function drives karyotype evolution in closely
843 related Malassezia species. *Elife* **9**.

844 Sanyal K, Baum M, Carbon J. 2004. Centromeric DNA sequences in the pathogenic yeast *Candida albicans* are all
845 different and unique. *Proc Natl Acad Sci U S A* **101**: 11374-11379.

846 Schleiffer A, Maier M, Litos G, Lampert F, Hornung P, Mechtler K, Westermann S. 2012. CENP-T proteins are
847 conserved centromere receptors of the Ndc80 complex. *Nat Cell Biol* **14**: 604-613.

848 Schotanus K, Soyer JL, Connolly LR, Grandaubert J, Happel P, Smith KM, Freitag M, Stukenbrock EH. 2015.
849 Histone modifications rather than the novel regional centromeres of *Zymoseptoria tritici* distinguish core and
850 accessory chromosomes. *Epigenetics Chromatin* **8**: 41.

851 Scott KC, Bloom KS. 2014. Lessons learned from counting molecules: how to lure CENP-A into the kinetochore.
852 *Open Biol* **4**.

853 Shang WH, Hori T, Toyoda A, Kato J, Popendorf K, Sakakibara Y, Fujiyama A, Fukagawa T. 2010. Chickens
854 possess centromeres with both extended tandem repeats and short non-tandem-repetitive sequences. *Genome Res* **20**:
855 1219-1228.

Shen XX, Opulente DA, Kominek J, Zhou X, Steenwyk JL, Buh KV, Haase MAB, Wisecaver JH, Wang M, Doering DT et al. 2018. Tempo and Mode of Genome Evolution in the Budding Yeast Subphylum. *Cell* **175**: 1533-1545 e1520.

Sridhar S, Hori T, Nakagawa R, Fukagawa T, Sanyal K. 2021. Bridgin connects the outer kinetochore to centromeric chromatin. *Nat Commun* **12**: 146.

Sun X, Wahlstrom J, Karpen G. 1997. Molecular structure of a functional Drosophila centromere. *Cell* **91**: 1007-1019.

Talbert PB, Henikoff S. 2020. What makes a centromere? *Exp Cell Res*: 111895.

Tanaka K, Kitamura E, Kitamura Y, Tanaka TU. 2007. Molecular mechanisms of microtubule-dependent kinetochore transport toward spindle poles. *J Cell Biol* **178**: 269-281.

Thakur J, Sanyal K. 2011. The essentiality of the fungus-specific Dam1 complex is correlated with a one-kinetochore-one-microtubule interaction present throughout the cell cycle, independent of the nature of a centromere. *Eukaryot Cell* **10**: 1295-1305.

-. 2012. A coordinated interdependent protein circuitry stabilizes the kinetochore ensemble to protect CENP-A in the human pathogenic yeast Candida albicans. *PLoS Genet* **8**: e1002661.

Tien JF, Umbreit NT, Gestaut DR, Franck AD, Cooper J, Wordeman L, Gonen T, Asbury CL, Davis TN. 2010. Cooperation of the Dam1 and Ndc80 kinetochore complexes enhances microtubule coupling and is regulated by aurora B. *J Cell Biol* **189**: 713-723.

Umbreit NT, Miller MP, Tien JF, Ortola JC, Gui L, Lee KK, Biggins S, Asbury CL, Davis TN. 2014. Kinetochores require oligomerization of Dam1 complex to maintain microtubule attachments against tension and promote biorientation. *Nat Commun* **5**: 4951.

van Hooff JJE, Snel B, Kops G. 2017. Unique Phylogenetic Distributions of the Ska and Dam1 Complexes Support Functional Analogy and Suggest Multiple Parallel Displacements of Ska by Dam1. *Genome Biol Evol* **9**: 1295-1303.

Walstein K, Petrovic A, Pan D, Hagemeier B, Vogt D, Vetter IR, Musacchio A. 2021. Assembly principles and stoichiometry of a complete human kinetochore module. *Sci Adv* **7**.

Weir JR, Faesen AC, Klare K, Petrovic A, Basilico F, Fischbock J, Pentakota S, Keller J, Pesenti ME, Pan D et al. 2016. Insights from biochemical reconstitution into the architecture of human kinetochores. *Nature* **537**: 249-253.

Winey M, Mamay CL, O'Toole ET, Mastronarde DN, Giddings TH, Jr., McDonald KL, McIntosh JR. 1995. Three-dimensional ultrastructural analysis of the Saccharomyces cerevisiae mitotic spindle. *J Cell Biol* **129**: 1601-1615.

Wisniewski J, Hajj B, Chen J, Mizuguchi G, Xiao H, Wei D, Dahan M, Wu C. 2014. Imaging the fate of histone Cse4 reveals de novo replacement in S phase and subsequent stable residence at centromeres. *Elife* **3**: e02203.

Wong J, Nakajima Y, Westermann S, Shang C, Kang JS, Goodner C, Houshmand P, Fields S, Chan CS, Drubin D et al. 2007. A protein interaction map of the mitotic spindle. *Mol Biol Cell* **18**: 3800-3809.

Yadav V, Sun S, Billmyre RB, Thimmappa BC, Shea T, Lintner R, Bakkeren G, Cuomo CA, Heitman J, Sanyal K. 2018. RNAi is a critical determinant of centromere evolution in closely related fungi. *Proc Natl Acad Sci U S A* **115**: 3108-3113.

Yadav V, Yang F, Reza MH, Liu S, Valent B, Sanyal K, Naqvi NI. 2019. Cellular dynamics and genomic identity of centromeres in cereal blast fungus. *mBio* **10**: e01581-01519.

894 Yan H, Talbert PB, Lee HR, Jett J, Henikoff S, Chen F, Jiang J. 2008. Intergenic locations of rice centromeric
895 chromatin. *PLoS Biol* **6**: e286.

896 Zelter A, Bonomi M, Kim JO, Umbreit NT, Hoopmann MR, Johnson R, Riffle M, Jaschob D, MacCoss MJ, Moritz
897 RL et al. 2015. The molecular architecture of the Dam1 kinetochore complex is defined by cross-linking based
898 structural modelling. *Nat Commun* **6**: 8673.

899

Figures and figure legends

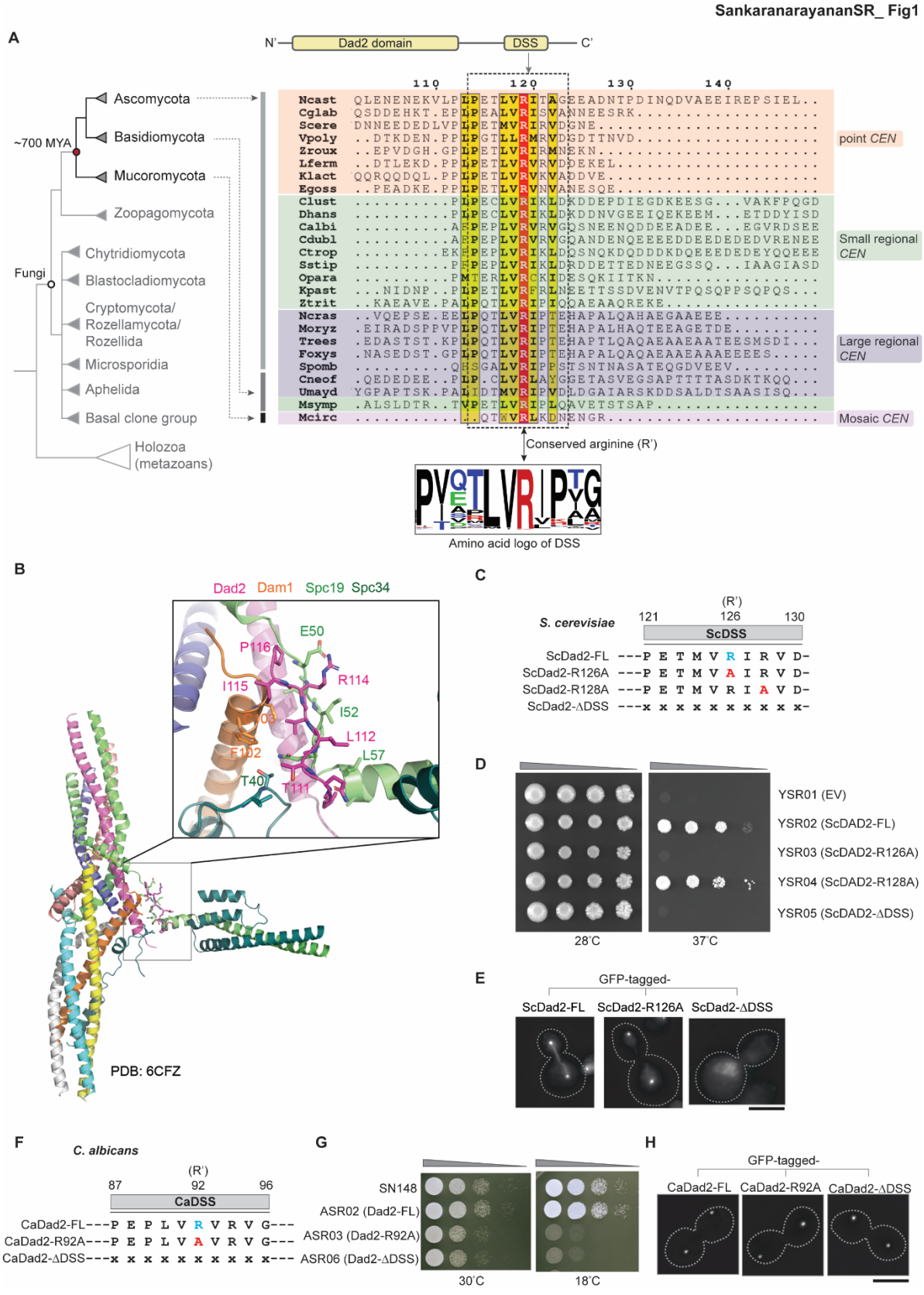

Figure 1. The functional significance of the conserved Dad2 signature sequence (DSS) motif is dependent on the length of centromeric chromatin. (A) *Top*, schematic of the Dad2 protein family indicating the known Dad2 domain (PF08654) at the N-terminus as well as a previously unknown conserved motif at the C-terminus. *Bottom*, the cladogram represents the relative phylogenetic position of major fungal phyla such as Ascomycota, Basidiomycota, and Mucoromycota and the corresponding species belong to them. The time of divergence of Mucoromycota from the common ancestor it shared with Ascomycota and Basidiomycota is based on (Berbee et al. 2017). A representative alignment of Dad2 amino acid sequences highlighting the conservation of the DSS and its conserved arginine residue (R') across species with known centromere structures is shown. The consensus sequence of the DSS represented as an amino acid logo was generated from a multiple sequence alignment of 466 Dad2 sequences (Supplementary table 1). The height of each amino acid indicates its probability of occurrence at the specific position. Amino acids are color-coded based on the inherent charge contributed by the side chain: black, neutral; red, positive; green, negative; blue, polar. (B) Cartoon representation of the three-dimensional structure of the DASH/Dam1 complex determined by Jenni and Harrison, 2018 (PDB: 6CFZ). The inset shows the close-up views of the Dad2 DSS motif and segments of Dam1, Spc19, and Spc34 which are in close proximity to the DSS motif. Amino acid residues contacting the DSS motif are shown in stick representation. (C) The amino acid sequence of the DSS in *S. cerevisiae* Dad2 (ScDad2) depicting the conserved arginine residue (blue) is shown along with the mutants generated to study the function of the DSS in *S. cerevisiae*. (D) The full-length wild-type *DAD2* or with mutations in the DSS (121-130 aa in ScDad2) or a truncated version of *DAD2* lacking the DSS as mentioned in (B) were cloned into pRS313. These constructs were used to transform a temperature-sensitive *dad2* mutant CJY077 to express them as C-terminally GFP-tagged proteins. YSR01 corresponds to a control strain carrying the empty vector. Single colonies of the strains YSR01 through YSR05 were grown on CM-Leu-His media for 14 h at 26°C, serially diluted ten-fold, and spotted (10^5 to 10^2) on CM-Leu-His plates and incubated at 26°C and 37°C respectively. Plates were photographed after 72 h of incubation. (E) Fluorescence microscopic images showing the localization of indicated versions of Dad2-GFP in cells grown for 4 h at 37°C. Scale bar, 5 µm. (F) The DSS sequences in the indicated strains generated to assay for the role of the DSS and the conserved arginine residue (R') in *C. albicans*. x indicates absence of an amino acid residue. (G) Spot dilution assay performed with the indicated strains grown in YPDU for 14 h at 30°C. Cells

933 were serially diluted ten-fold, spotted on YPDU plates (10^5 to 10^2 cells), incubated at 30°C and
934 18°C, and imaged after 36 h and 48 h respectively. (H) Fluorescence microscopy images of *C.*
935 *albicans* cells expressing the indicated versions of Dad2-GFP after logarithmic growth in YPDU
936 at 30°C. Scale bar, 5 μm

937

SankaranarayananSR_ Fig2

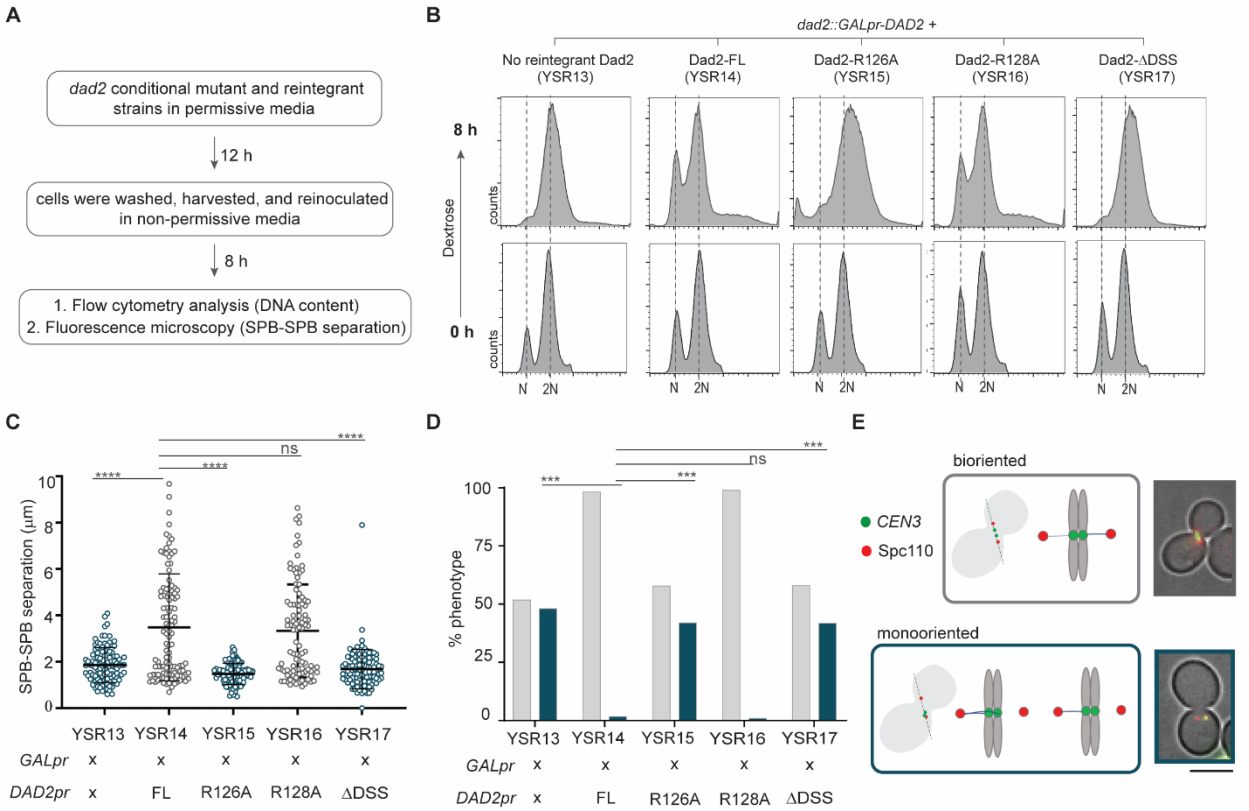

938

939

940 **Figure 2. Alanine substitution of the conserved arginine R126 in Dad2 results in defective**
941 **spindle dynamics and monooriented kinetochores in *S. cerevisiae*.** (A) Flowchart of the
942 experimental design followed to study the contribution of the DSS in Dad2 function in *S. cerevisiae*
943 using the strains YSR13 through YSR17. (B) Histograms indicate the distribution of cells with N
944 and 2N DNA content (*x*-axis) in the *dad2* conditional mutant strain YSR13 and the reintegrant
945 strains YSR14 through YSR17 upon depletion of endogenous Dad2 for 8 h followed by propidium
946 iodide staining. (C) The Dad2 conditional mutant strain and the reintegrant strains were analyzed
947 by fluorescence microscopy to study spindle dynamics (using Spc110-mCherry) in each of these
948 strains. The spindle length derived from the SPB-SPB distance (*y*-axis) in each of these strains
949 upon depletion of endogenous Dad2 for 8 h is shown. Only large-budded cells with BI>0.65 were
950 used for analysis. Statistical significance was tested by one-way ANOVA (****, $p<0.0001$,
951 $n>100$). (D) The kinetochore orientation in the indicated strains were studied by colocalizing
952 Spc110-mCherry with *CEN3*-GFP. The bar plots represent the proportion of cells with bioriented
953 (grey) or monooriented kinetochores (*CEN3*-GFP) (blue) in each strain. Cells with two *CEN3*-
954 GFP puncta between the two SPBs were considered bioriented, and those with only one *CEN3*-
955 GFP punctum closer to one of the two SPBs were considered monooriented. Only large-budded
956 cells with BI>0.65 were used for analysis. Statistical significance was tested by one-way ANOVA
957 (***, $p<0.001$, $n>100$). (E) Schematic representation of bioriented and monooriented kinetochore-
958 MT attachments is shown along with a representative microscopic image (*right*). Scale bar, 5 µm.

959

SankaranarayananSR_ Fig3

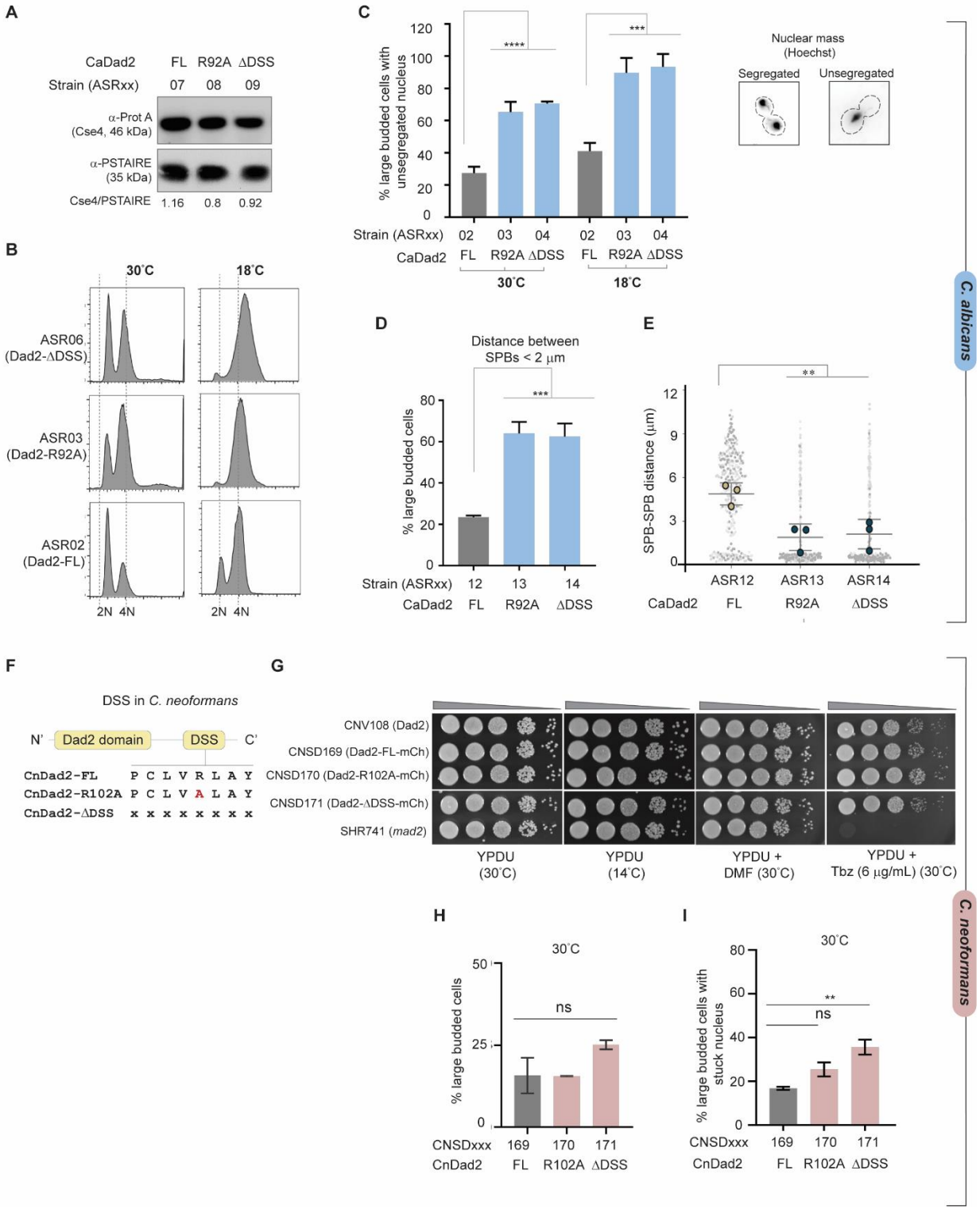

Figure 3. Alanine substitution of the conserved arginine residue in the DSS is tolerated in *C. albicans* and *C. neoformans*. (A) The cellular levels of Cse4 in strains ASR07 through ASR09 expressing the indicated versions of Dad2 along with a Protein-A-tagged Cse4. Whole-cell extracts were prepared from cells grown at 30°C and probed with anti-Protein A and anti-PSTAIRE antibodies. The relative Cse4 level normalized to PSTAIRE in each sample is indicated below the blot. (B) Strains expressing indicated versions of Dad2 were grown in YPDU overnight at 30°C. Cells were reinoculated in YPDU to 0.2 OD_{600} and allowed to grow for two generations at 30°C and 18°C. Histograms depict the distribution of cells with 2N and 4N DNA content (*x*-axis) after flow cytometry analysis. (C) The bar graph indicates the proportion of large-budded cells (BI >0.65) showing unsegregated nuclei in strains ASR02 through ASR04, expressing indicated versions of Dad2, after growth at 30°C and 18°C as shown. Data from three independent experiments were used to generate the plot, and statistical significance was tested by one-way ANOVA (*****p<0.0001, ***p<0.0003*, n>100). A representative image of segregated and unsegregated nuclear mass is shown (*right*). (D) Strains ASR12 through ASR14, expressing indicated versions of Dad2 and Tub4-mCherry, were grown to log phase in YPDU at 30°C and imaged using a fluorescence microscope. The percentage of large-budded cells (BI>0.65) showing closely placed SPBs (< 2 μm) in each strain is plotted. (E) The scatter plot shows the distance between the SPBs in the strains ASR12 through ASR14. The gray circles represent data from three experiments, each colored with a different shade of gray. Circles with a black border represent the mean of each experiment, and the error bars indicate SD among the mean values. Only large-budded cells with BI>0.65 were included in the analysis. Data from three independent experiments was used to generate the plots. Statistical significance was tested by one-way ANOVA (***p<0.0008, **p<0.0095*, n>100). (F) Schematic depicts the position and sequence of amino acids in the DSS in *C. neoformans* Dad2 and the mutants generated (CnDad2-R102A and CnDad2-ΔDSS) to study the function of the conserved arginine in the DSS in this species. (G) Spot dilution assay performed with the indicated strains grown in YPDU for 14 h at 30°C. Cells were serially diluted ten-fold (10^5 to 10 cells) and spotted on YPDU plates with the indicated additives and incubated at 30°C. One YPDU plate was incubated at 14°C to test for cold sensitivity. Plates at 30°C were imaged 48 h post-incubation. The plate incubated at 14°C was imaged after 5 days. (H) The proportion of large-budded cells in strains CNSD169 through CNSD171 expressing CnDad2-FL, CnDad2-R102A, and CnDad2-ΔDSS after logarithmic growth at 30°C in YPDU as observed

994 under a microscope (n>100). (I) The percentage of large-budded cells with an unsegregated
995 nuclear mass is plotted for strains CNSD169 through CNSD171 (n>100, unpaired t-test with
996 Welch's correction, **, $p<0.01$).

997

SankaranarayananSR_ Fig4

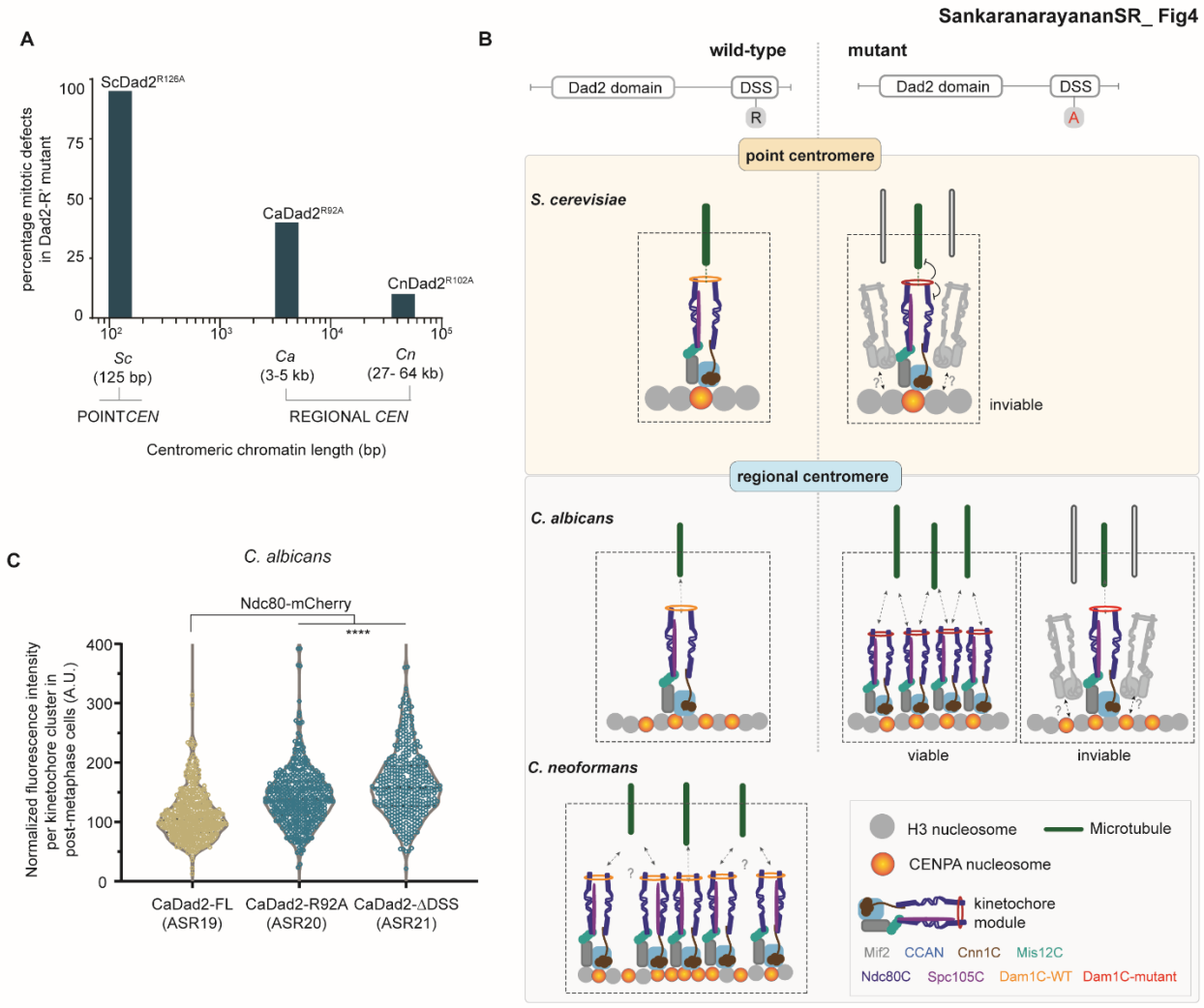

D

Organism	*CEN* structure	CENPA chromatin	CENPA nucleosomes/CEN	kMTs /Chr	Ref
S. cerevisiae	point	125 bp	1-2	1	Winey et al.,(1995)
C. albicans	small regional	3-5 kb	4	1	Joglekar et al.,(2008)
S. pombe	large regional	~10 kb	10-15	2-3	Ding et al.,(1993)
G. gallus	large regional	>30 kb	ND	~4	Ribeiro et al.,(2009)
H. sapiens	large regional	0.3-5 Mb	~100	12-23	Wendell et al.,(1993)
C. neoformans	large regional	27-64 kb	>10	>2	proposed in this study

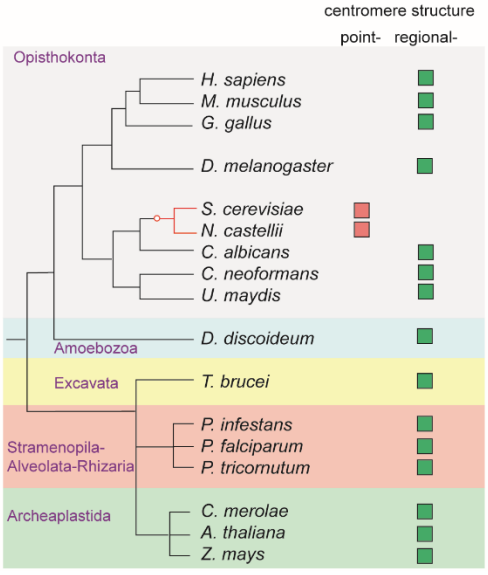

Figure 4. The tolerance towards alanine substitution of the conserved arginine in the DSS is dependent on the length of centromeric chromatin. (A) Summary of the alanine substitution mutant phenotype across the three fungal species tested in this study. The length of centromeric chromatin of each species is mentioned in the *x*-axis. The diminishing severity of the mutant phenotype in each of the species studied is represented in the *y*-axis as the frequency of cells showing defective segregation in the form of an unsegregated nuclear mass and/or a short mitotic spindle. Abbreviations in the *x*-axis indicate the following: Sc, *S. cerevisiae*; Ca, *C. albicans*; and Cn, *C. neoformans*. (B) A model to explain the effect of mutations in the DSS in organisms with point centromeres versus those with regional centromeres. The kinetochore formed on a single CENPA nucleosome binds to a MT during chromosome segregation in organisms with point centromeres. Mutations compromising the efficiency of this interaction can result in viability loss. In the case of regional centromeres, represented by *C. albicans*, the centromeres possess additional CENPA nucleosomes apart from the one that binds to a MT (Joglekar et al. 2008; Burrack et al. 2011; Thakur and Sanyal 2011). Cells that can recruit excess outer kinetochore proteins often enable additional kMTs to bind to a chromosome facilitating chromosome segregation even with a mutant kinetochore. The subset of cells unable to recruit excess kinetochore proteins/kMTs eventually lose viability. The inherent property of *C. neoformans* centromeres to bind multiple microtubules as predicted from the size of the centromeric chromatin is shown. This configuration makes the conserved arginine residue in the DSS dispensable for viability in *C. neoformans*. (C) *C. albicans* strains ASR19 through ASR21, expressing indicated versions of Dad2 and Ndc80-mCherry, were grown to log phase at 30°C, washed, and observed under a fluorescence microscope. The normalized fluorescence intensity of Ndc80-mCherry per kinetochore cluster in each strain (*x*-axis) is plotted (*y*-axis). Data from three experiments covering > 350 kinetochore clusters were used to generate the violin plot. Statistical significance was tested by one-way ANOVA (****, $p<0.0001$). (D) A table summarizing experimentally validated centromeric features of common model organisms. These centromeric properties were used to predict the number of CENPA nucleosomes and the number of associated kMTs (red letters) in *C. neoformans*. (E) The prevalence of regional centromere structure among eukaryotes is illustrated with a cladogram depicting major eukaryotic lineages and the occurrence of point and regional centromere structures in each of them. The cladogram was generated with species representative

of each eukaryotic supergroup (adapted from Van Hoofe et al. 2017). The red circle in the cladogram marks the only known origin of point centromeres.